



HyGAL : Characterizing the Galactic ISM

SOFIA observations of atomic O, OH, and CH

- The proxy of H₂ gas in the ISM & Oxygen

Wonju Kim

I. Physikalisches Institut, Universität zu Köln

Heritage of SOFIA – Scientific Highlights and Future Perspectives, Stuttgart

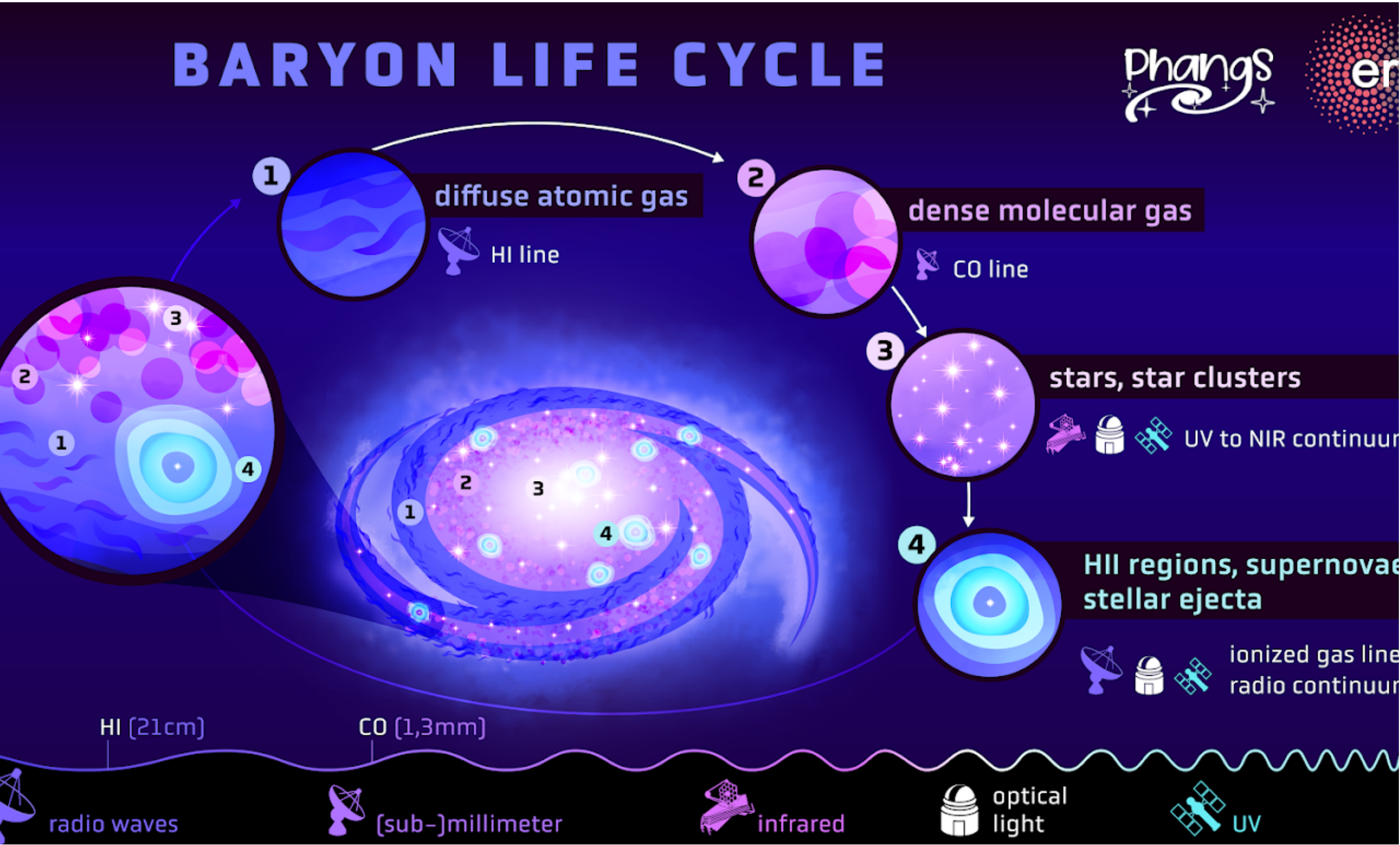
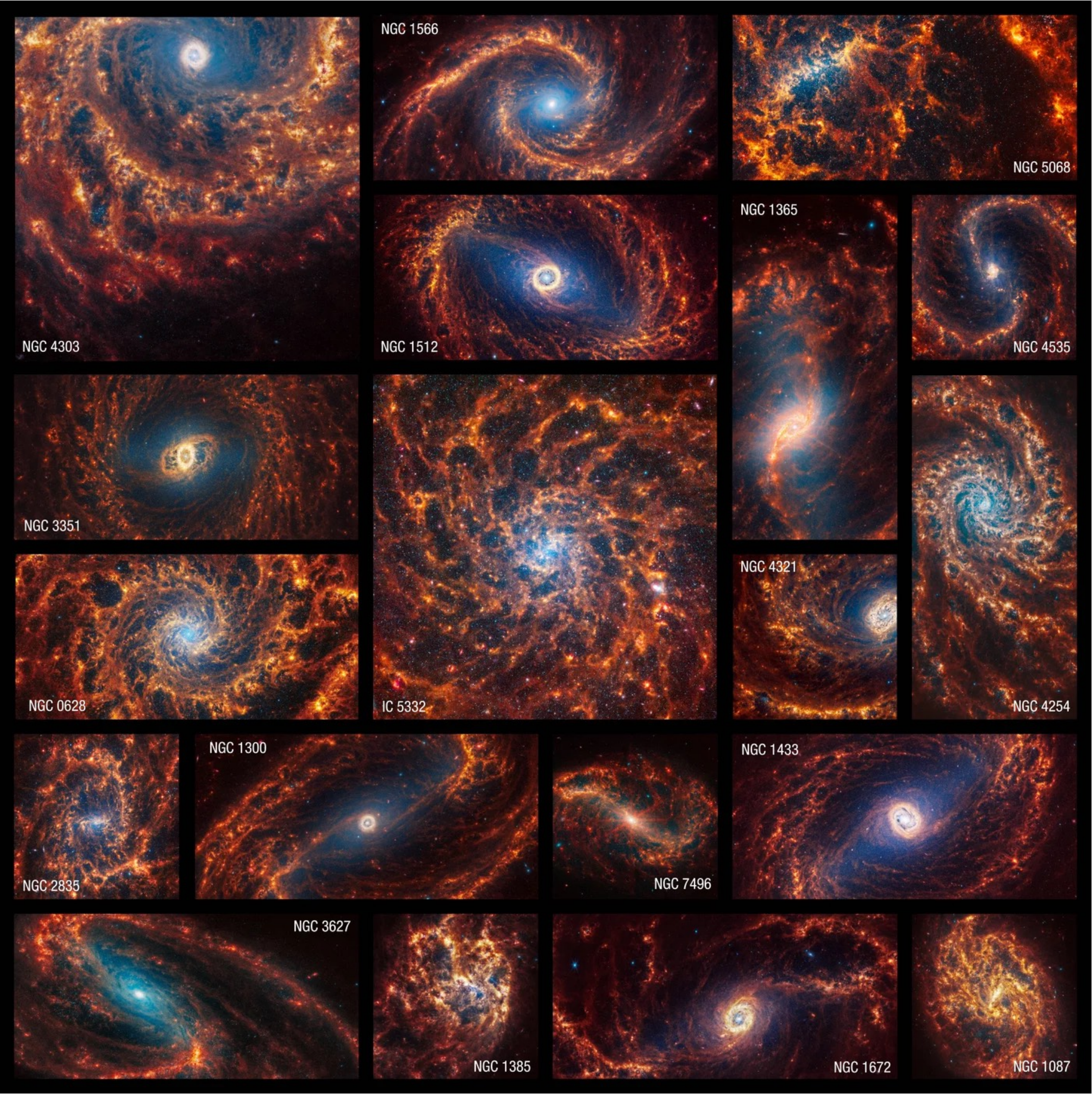


PIs: D. Neufeld (JHU), P. Schilke (UzK)
A. M. Jacob, A. Sterberg, B. Godard, D. Lis, D. Elia, M. Gerin, M. Wolfire, N. Indriolo, H. Wiesemeyer, V. Ossenkopf-Okada, S. Bialy, D. Seifried, P. Sonnetrucker, V. Valdivia, S. Walch, F. Wyrowski, K. M. Menten, M. Busch, M. R. Rugel, A. Sánchez-Monge, R. Higgins, E. Falgarone, P. Hennebelle, S. Molinari



- Perfect laboratory to study the formation of molecular gas
- Understanding diffuse and translucent clouds helps understanding chemical evolution of dense molecular clouds.

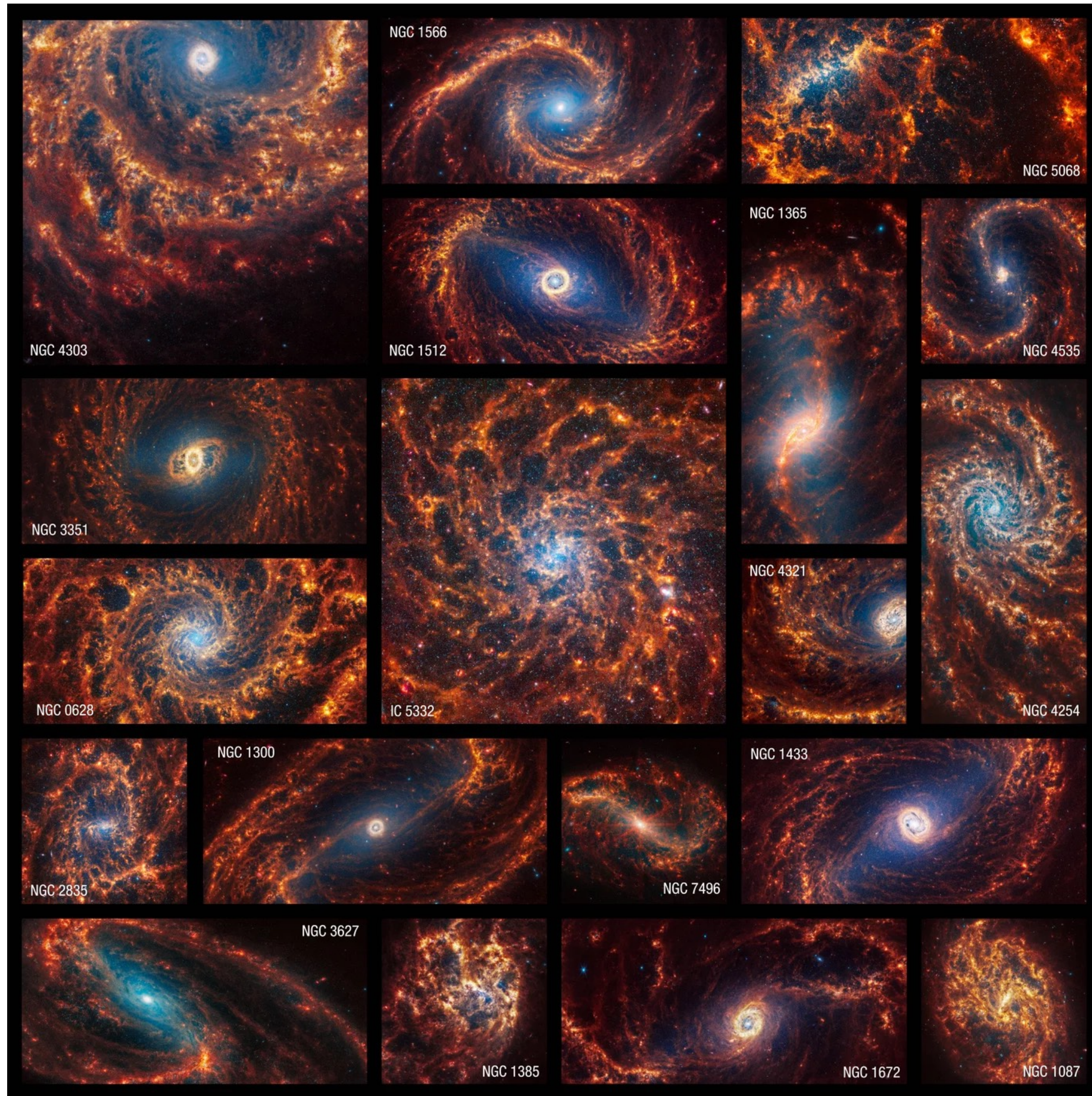




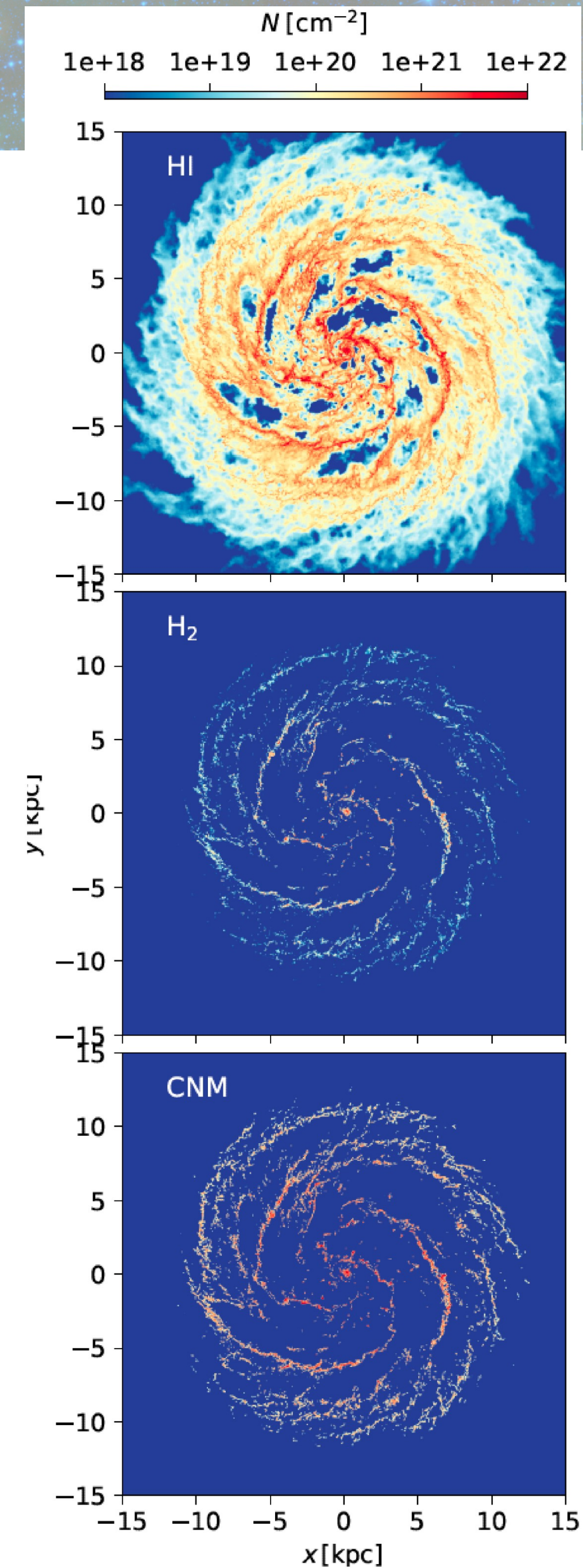
(Credit for both images: Phangs collaboration)

Life cycle of the interstellar medium

3



(Credit for both images: Phangs collaboration)



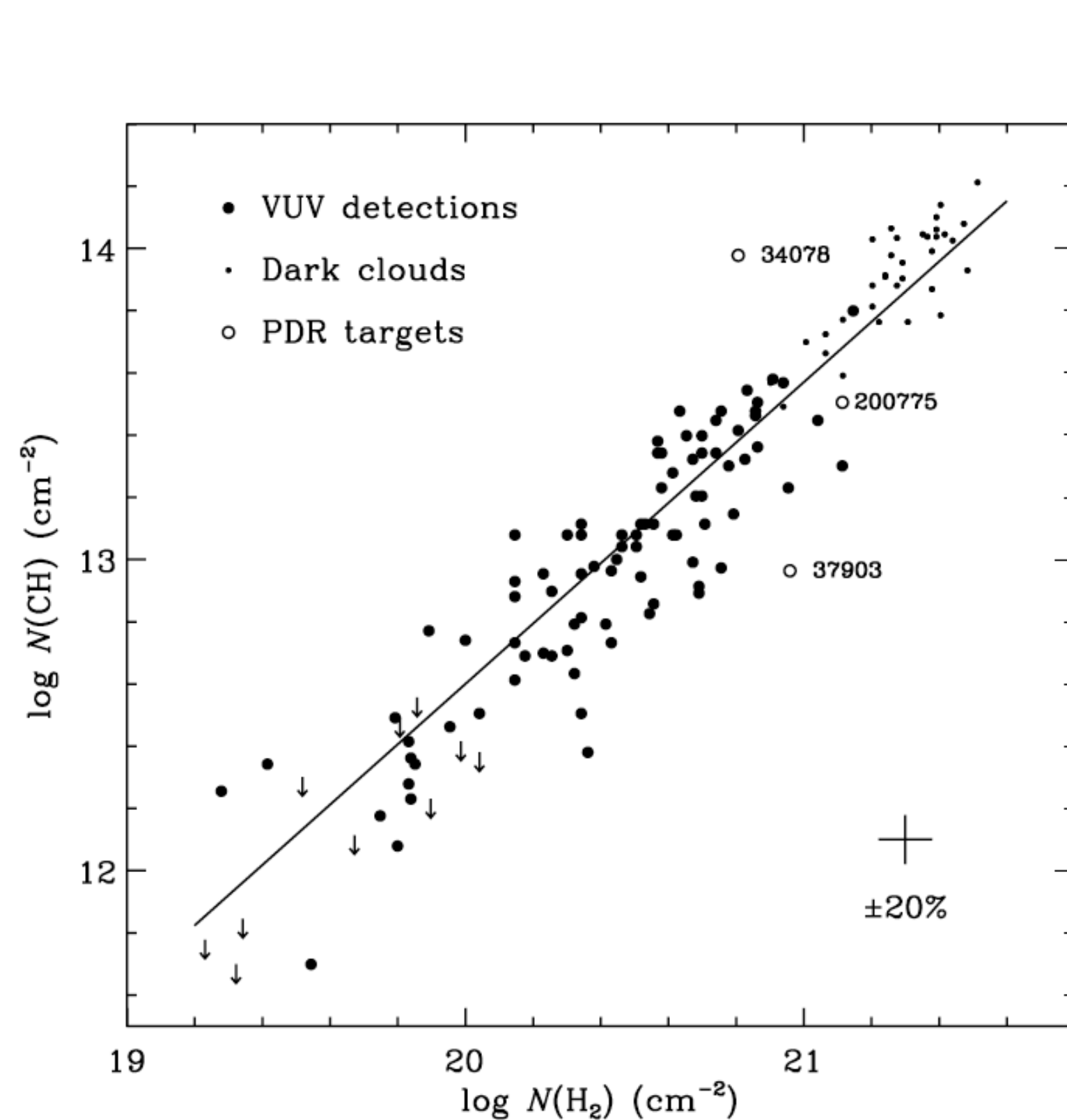
(Rowan et al. 2024)

- Simulation studies show a strong correlation between H₂ and CNM.
- HI gas traced by HI 21 cm transition.
- There is no direct tracer of H₂ in the cold ISM.
 - ➔ Need for the **proxy of H₂**!
 - ➔ Even tracing **CO-dark gas**.

CH and OH as the proxy of H₂

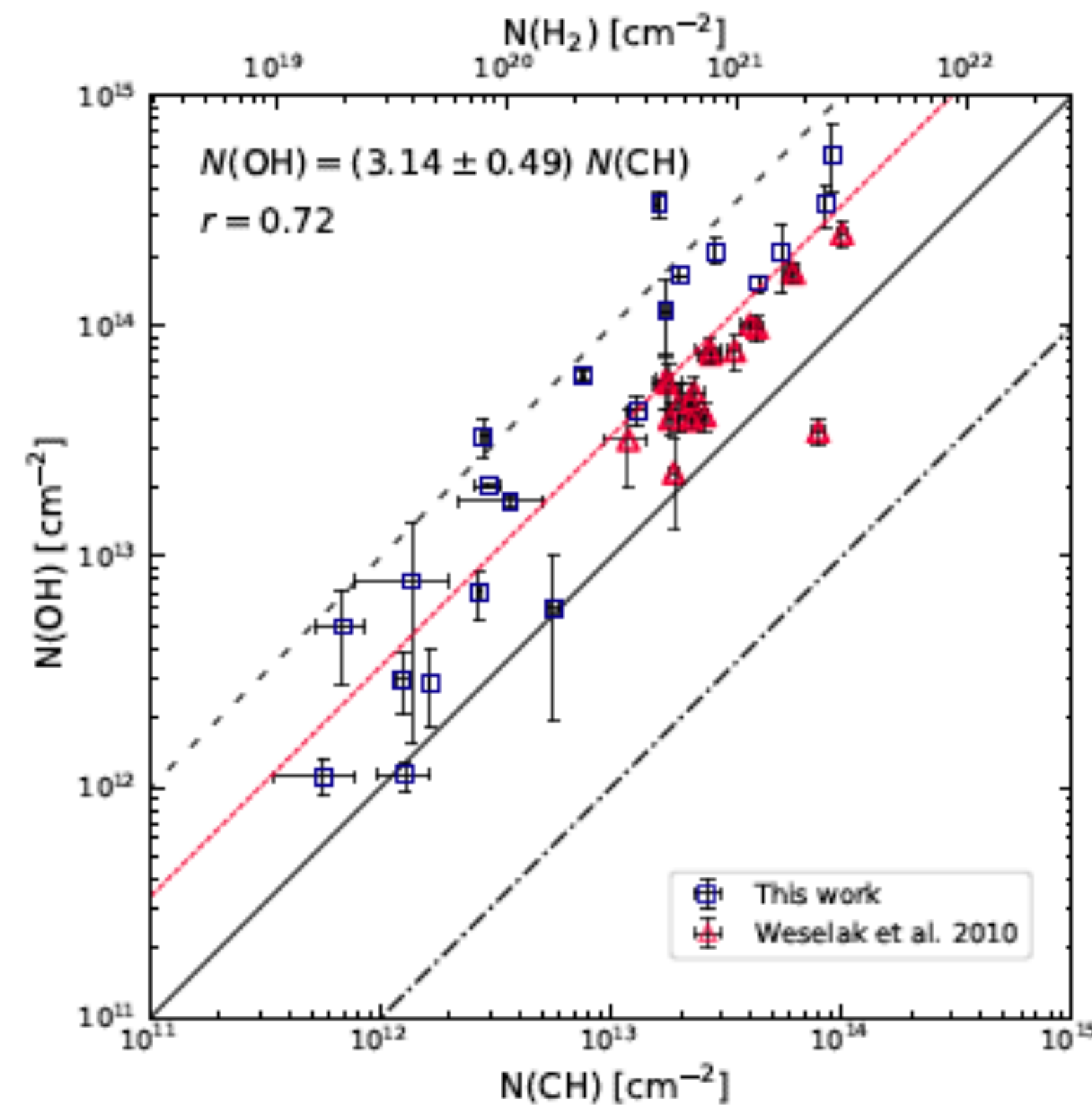
4

HF, CH, C₂H, OH, and HCO⁺ : excellent tracers of H₂ in diffuse clouds (e.g., Sheffer et al. 2008; Gerin et al. 2019; Jacob et al. 2019) without dust absorption at millimeter and submillimeter wavelengths.

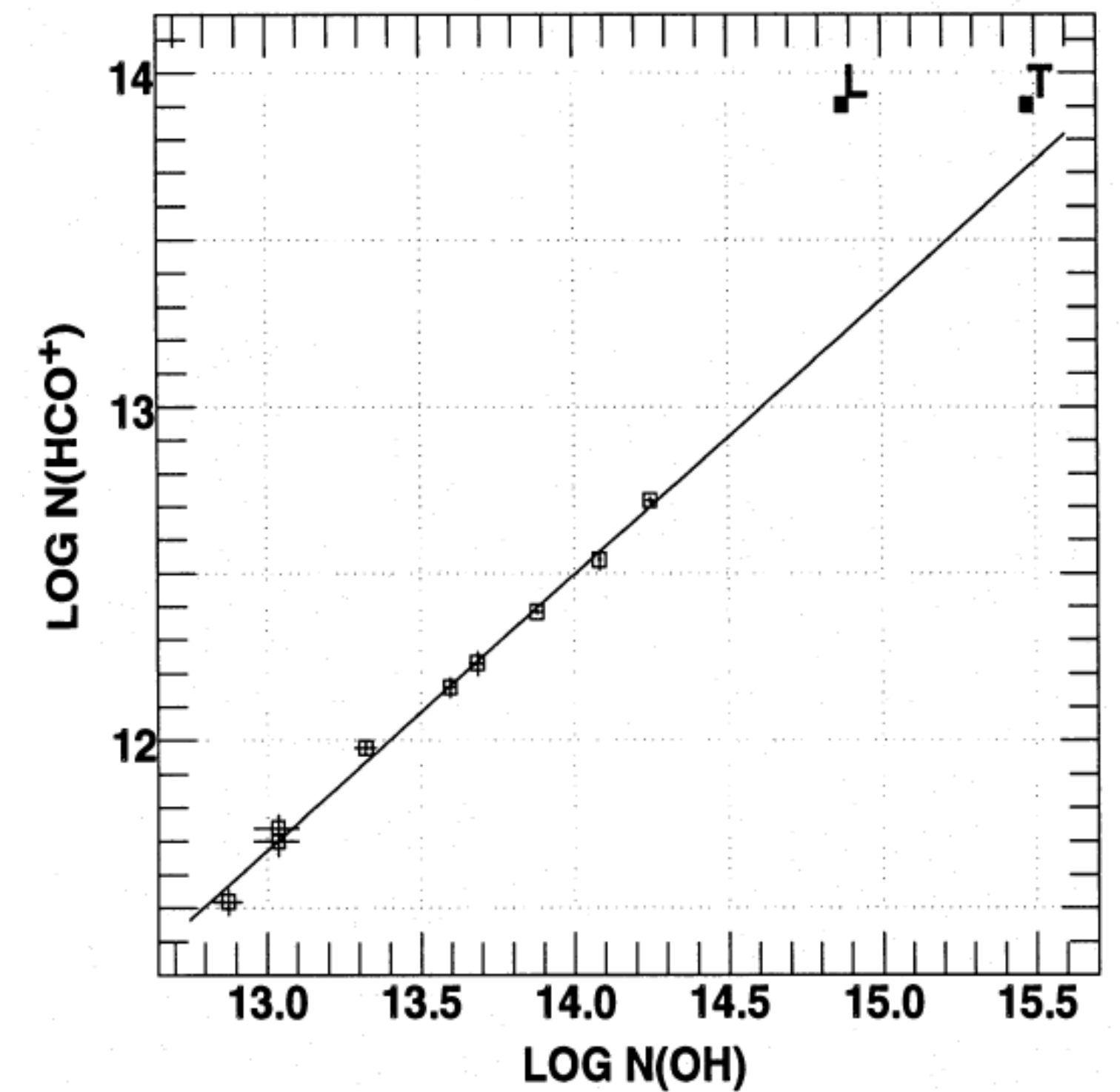


$$N(\text{CH})/N(\text{H}_2) = 3.5 \times 10^{-8}$$

(Sheffer et al. 2008)



(Jacob et al. 2019)

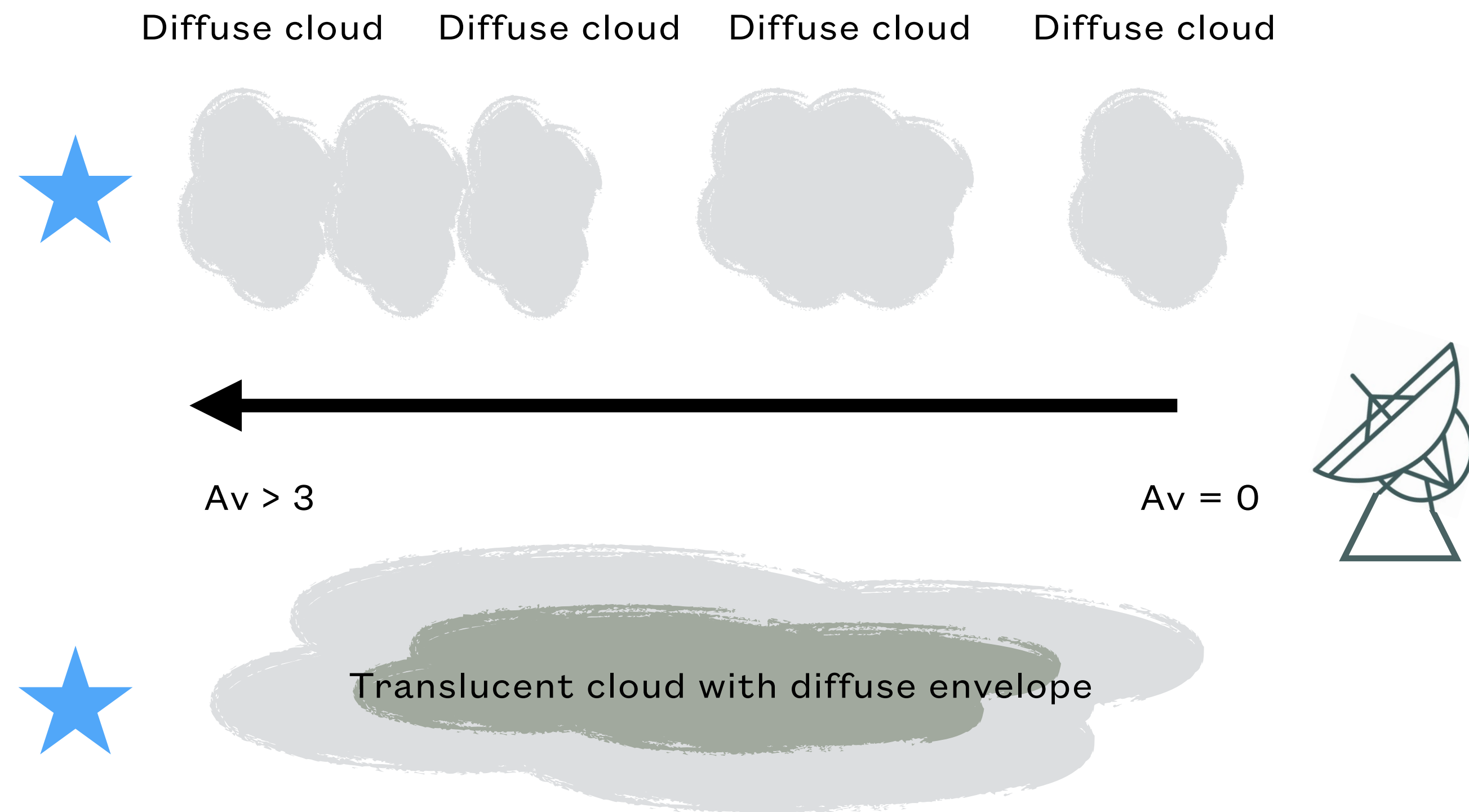


(Lucas & Liszt 1996)

Diffuse and translucent clouds

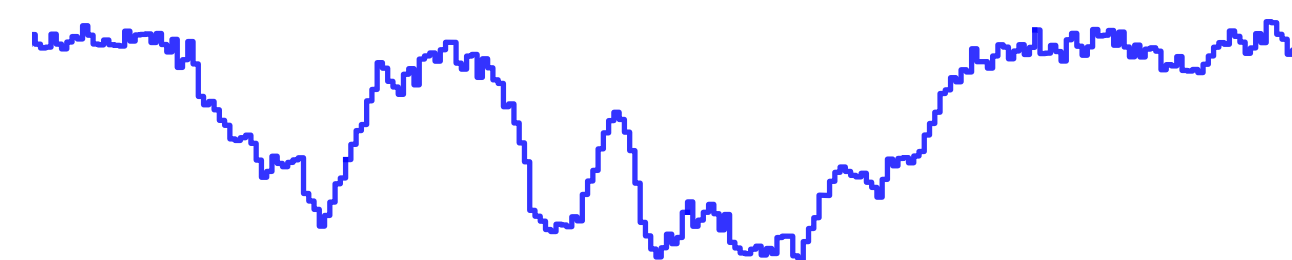
From observational point view

5

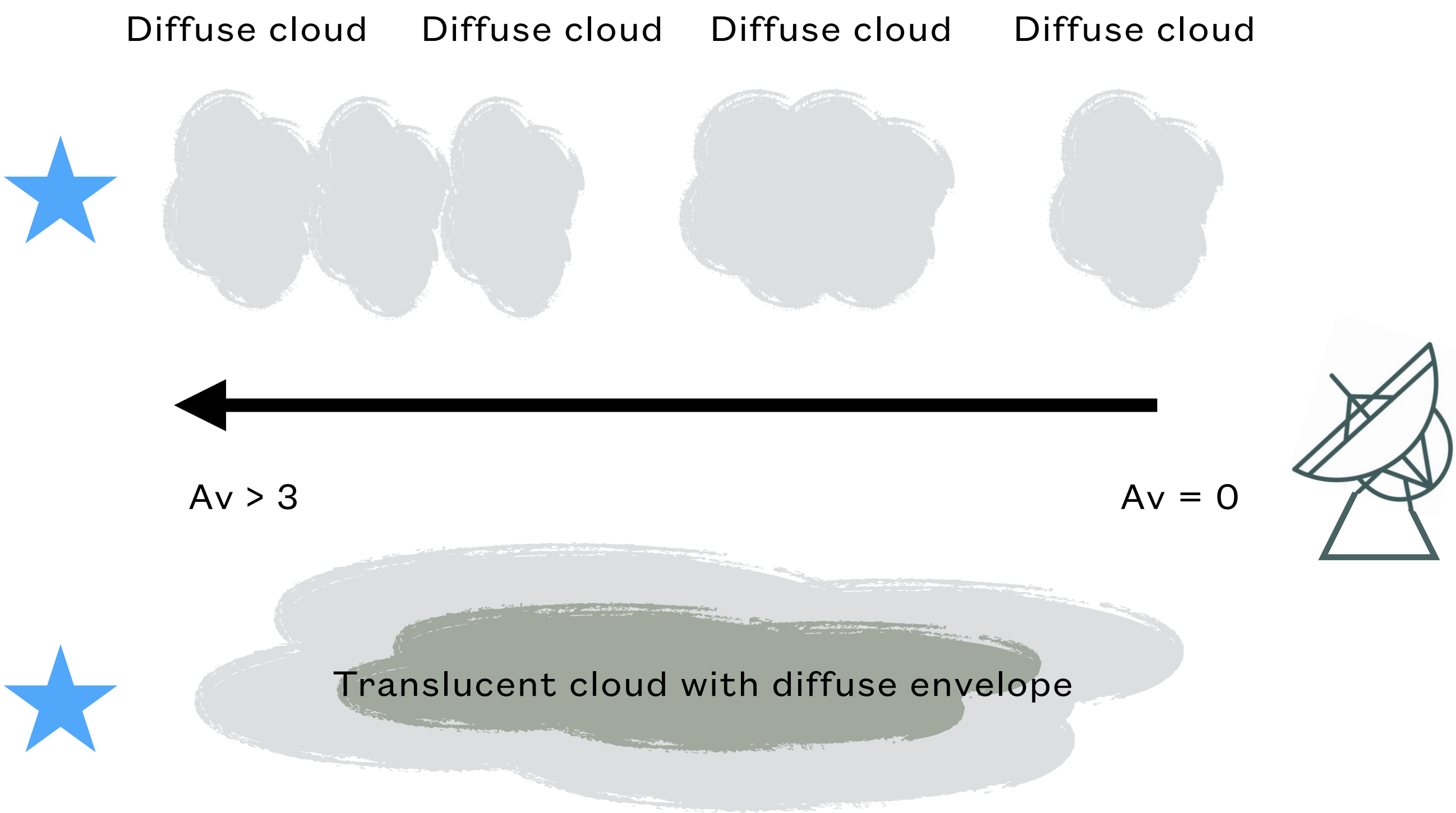


If A_v is only known, the total integrated atomic or molecular hydrogen fractions are probably similar for these two cases.

But we will not have the same observational results toward these sight-lines!

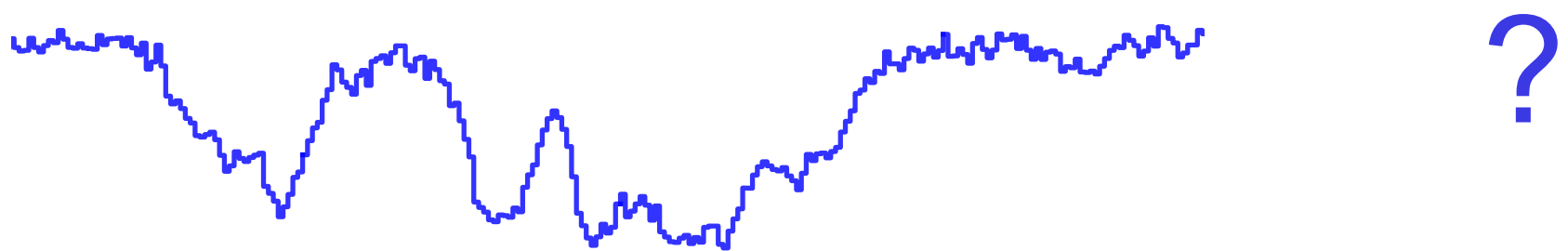


?



If A_v is only known, the total integrated atomic or molecular hydrogen fractions are probably similar for these two cases.

But we will not have the same observational results toward these sight-lines!

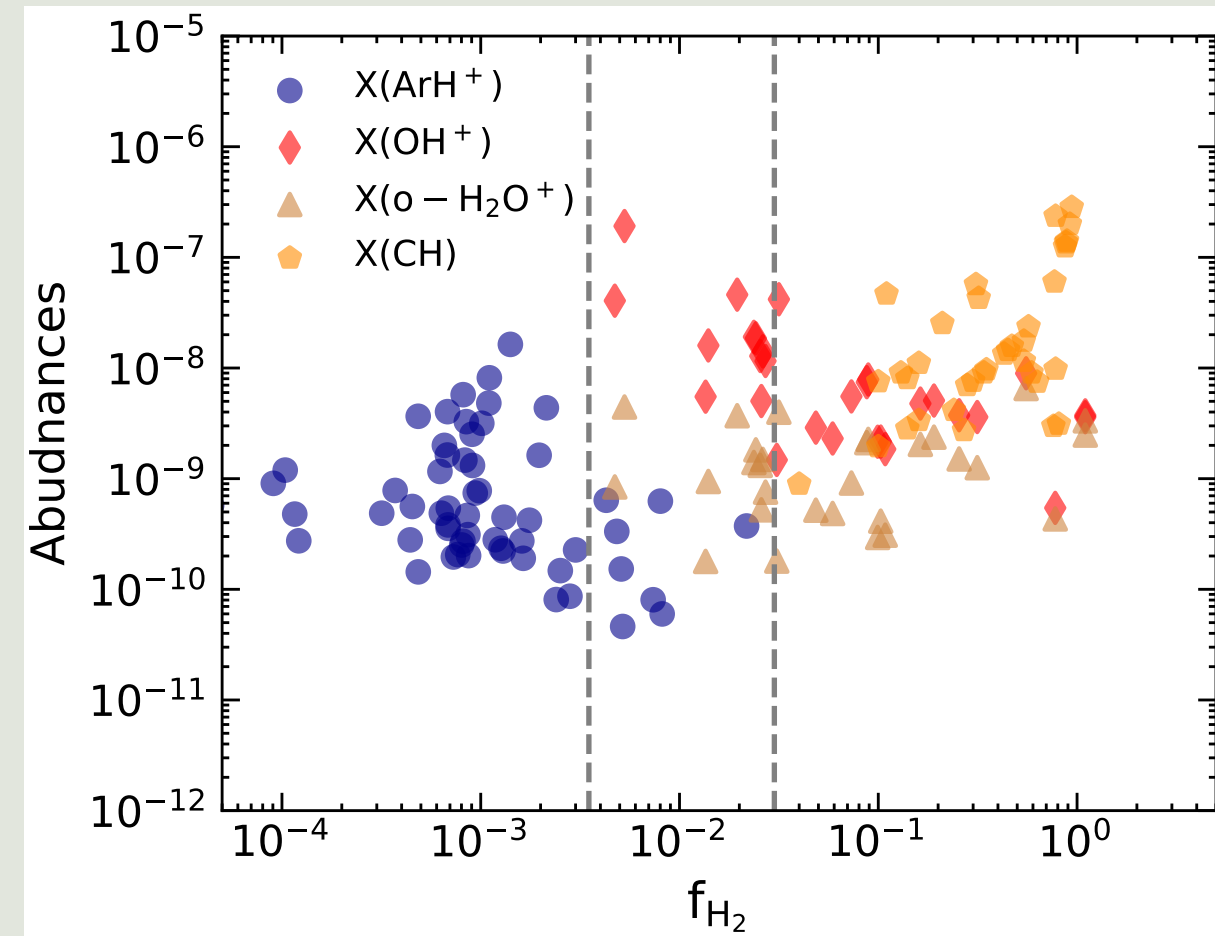


The primary reservoirs of gas-phase carbon, as well as $f_n(\text{H}_2)$, change from diffuse clouds to translucent clouds.

Snow et al. (2006)

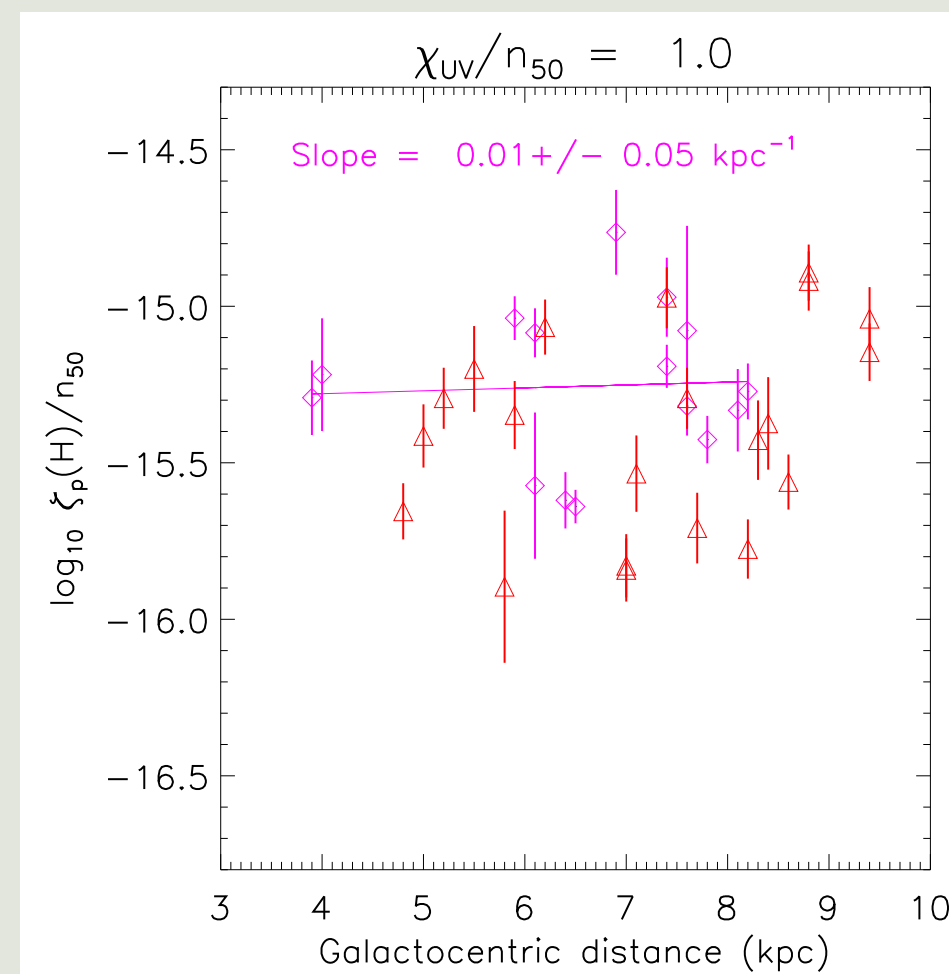
	Diffuse Atomic	Diffuse Molecular	Translucent	Dense Molecular
Defining Characteristic	$f_n^{\text{H}_2} < 0.1$	$f_n^{\text{H}_2} > 0.1$ $f_n^{\text{C}^+} > 0.5$	$f_n^{\text{C}^+} < 0.5$ $f_n^{\text{CO}} < 0.9$	$f_n^{\text{CO}} > 0.9$
A_V (min.)	0	~ 0.2	$\sim 1\text{--}2$	$\sim 5\text{--}10$
Typ. n_{H} (cm^{-3})	10–100	100–500	500–5000?	$> 10^4$
Typ. T (K)	30–100	30–100	15–50?	10–50
Observational Techniques	UV/Vis H I 21-cm	UV/Vis IR abs mm abs	Vis (UV?) IR abs mm abs/em	IR abs mm em

GOAL : To understand how molecular clouds are formed and the chemical and physical processes leading to the transitions from atomic to molecular gas (see [HyGAL I paper](#); [Jacob et al. 2022](#) for overview of the program and details).



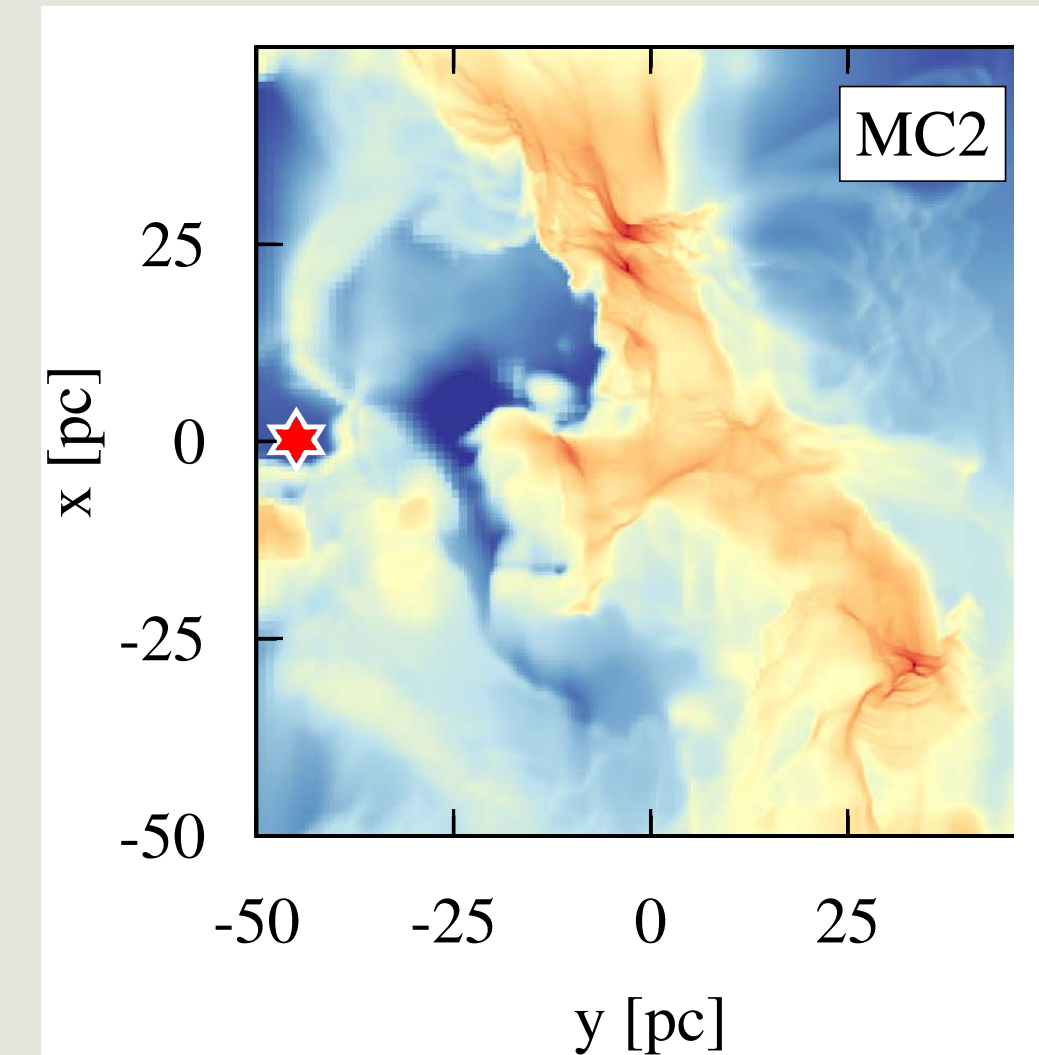
(Jacob et al. 2020)

Distribution of molecular fraction in different ISM phases



(Neufeld & Wolfire 2017)

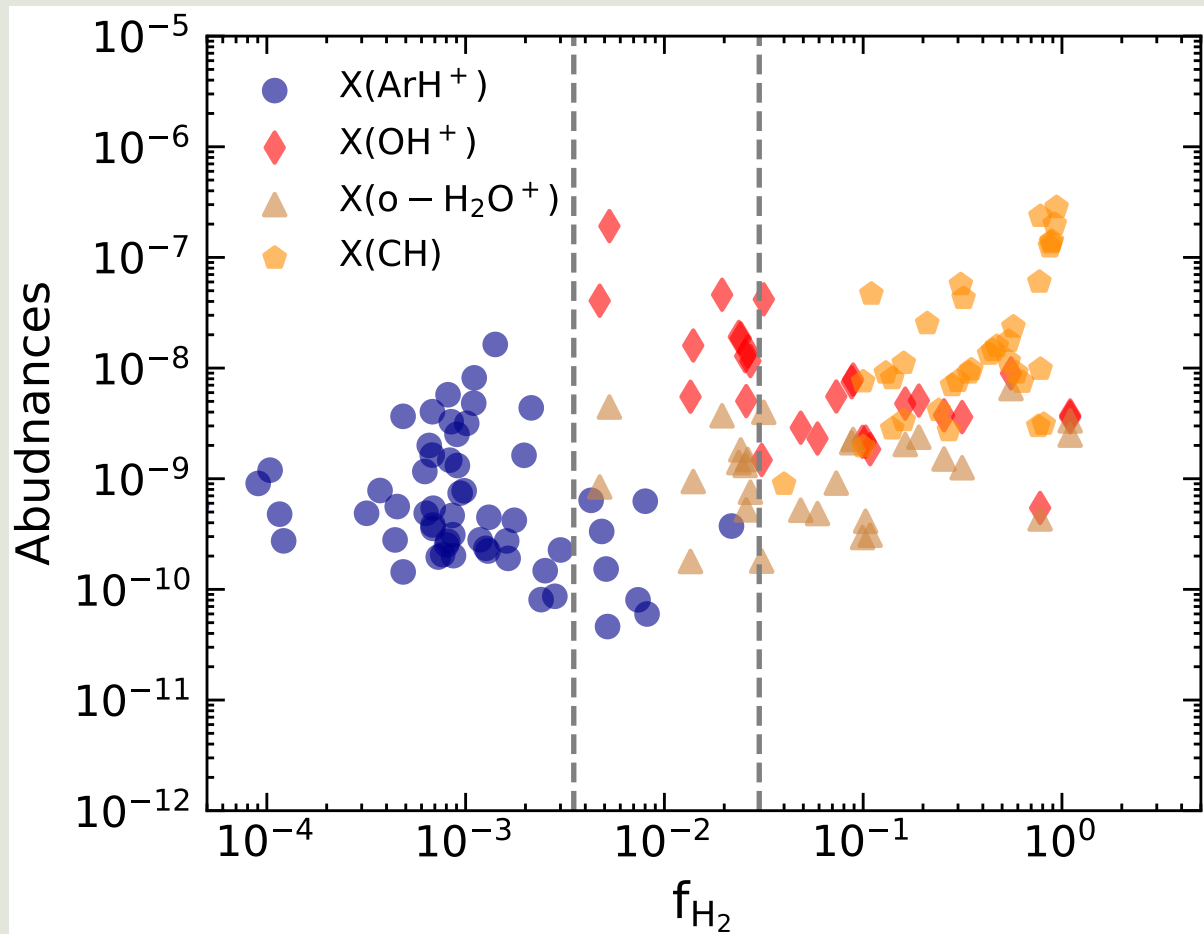
Variation in cosmic-ray ionisation rate across Galactocentric distances



(Seifried et al. 2018)

Nature of turbulence in the ISM and its dissipation

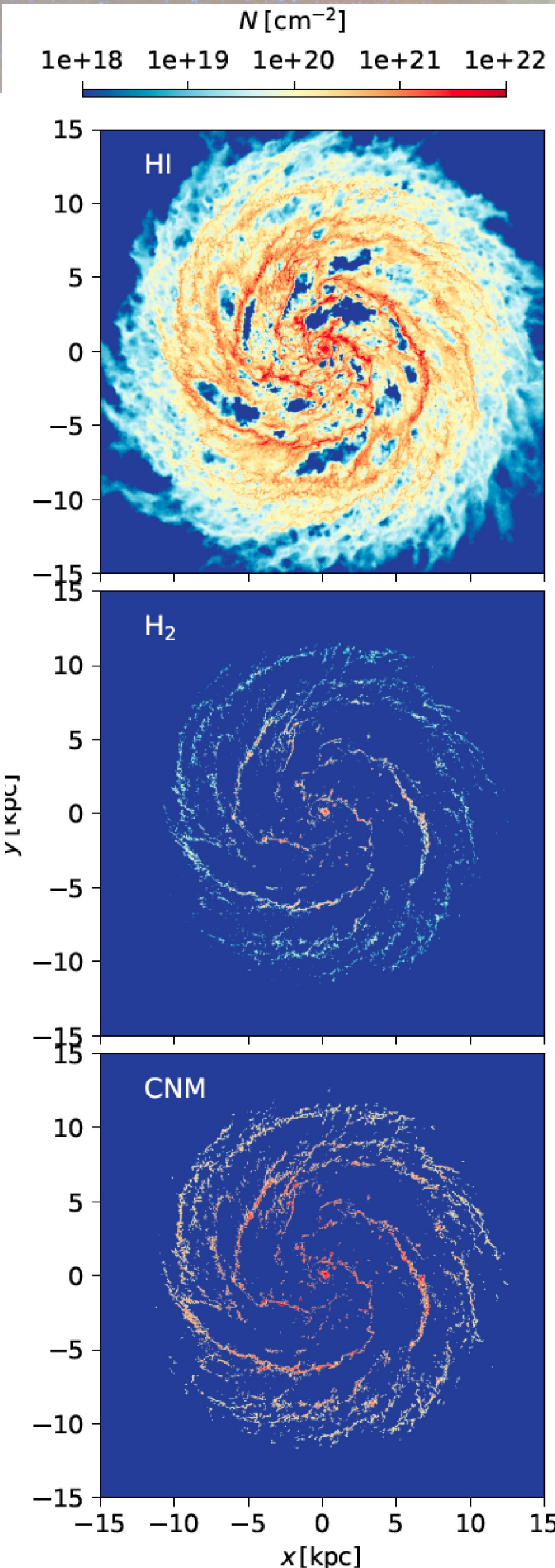
HyGAL will characterise following three main properties of the ISM:



(Jacob et al. 2020)

- Investigating the distribution of molecular fractions in different ISM phases in the Milky Way
 - Is it connected to the structure of the Milky Way, or local environment, or both?
 - Are there abundance variations for carbon or oxygen-bearing species?

	Diffuse Atomic	Diffuse Molecular	Translucent	Dense Molecular
Defining Characteristic	$f_{\text{H}_2}^{\text{n}} < 0.1$	$f_{\text{H}_2}^{\text{n}} > 0.1$ $f_{\text{C}^+}^{\text{n}} > 0.5$	$f_{\text{C}^+}^{\text{n}} < 0.5$ $f_{\text{CO}}^{\text{n}} < 0.9$	$f_{\text{CO}}^{\text{n}} > 0.9$
A_V (min.)	0	~ 0.2	$\sim 1-2$	$\sim 5-10$
Typ. n_{H} (cm^{-3})	10–100	100–500	500–5000?	$> 10^4$
Typ. T (K)	30–100	30–100	15–50?	10–50
Observational Techniques	UV/Vis H I 21-cm	UV/Vis IR abs mm abs	Vis (UV?) IR abs mm abs/em	IR abs mm em

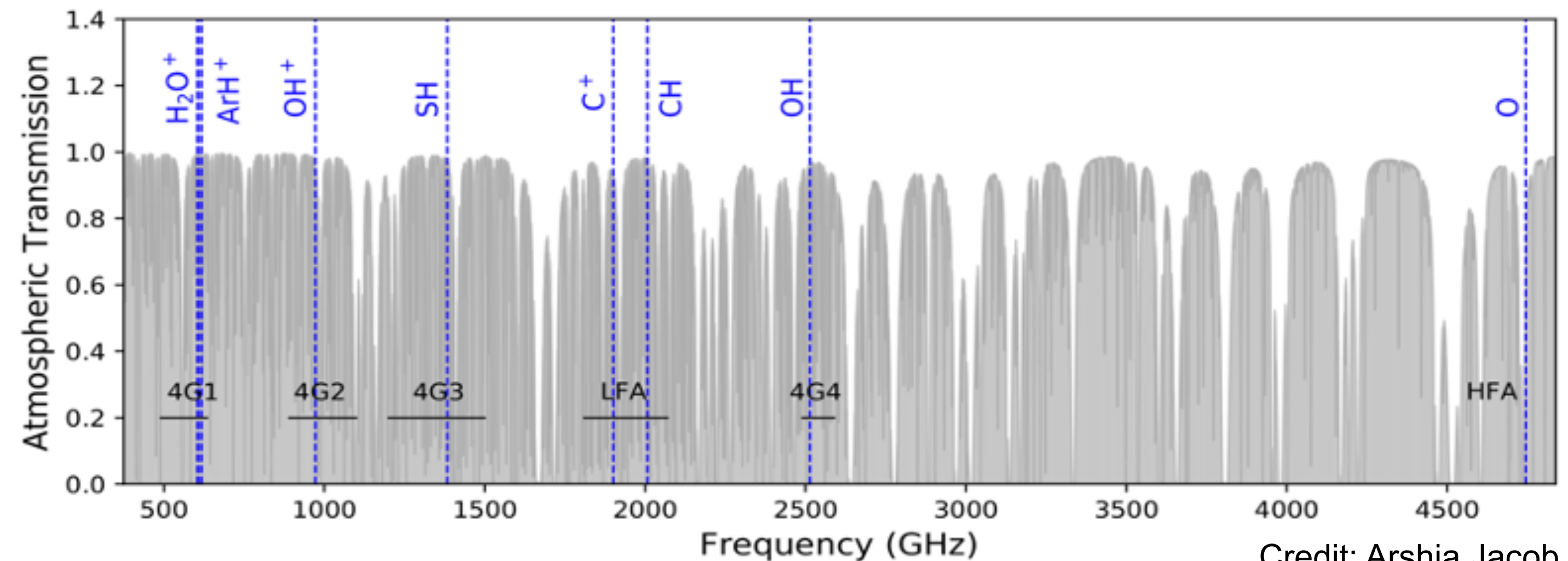


Target species:

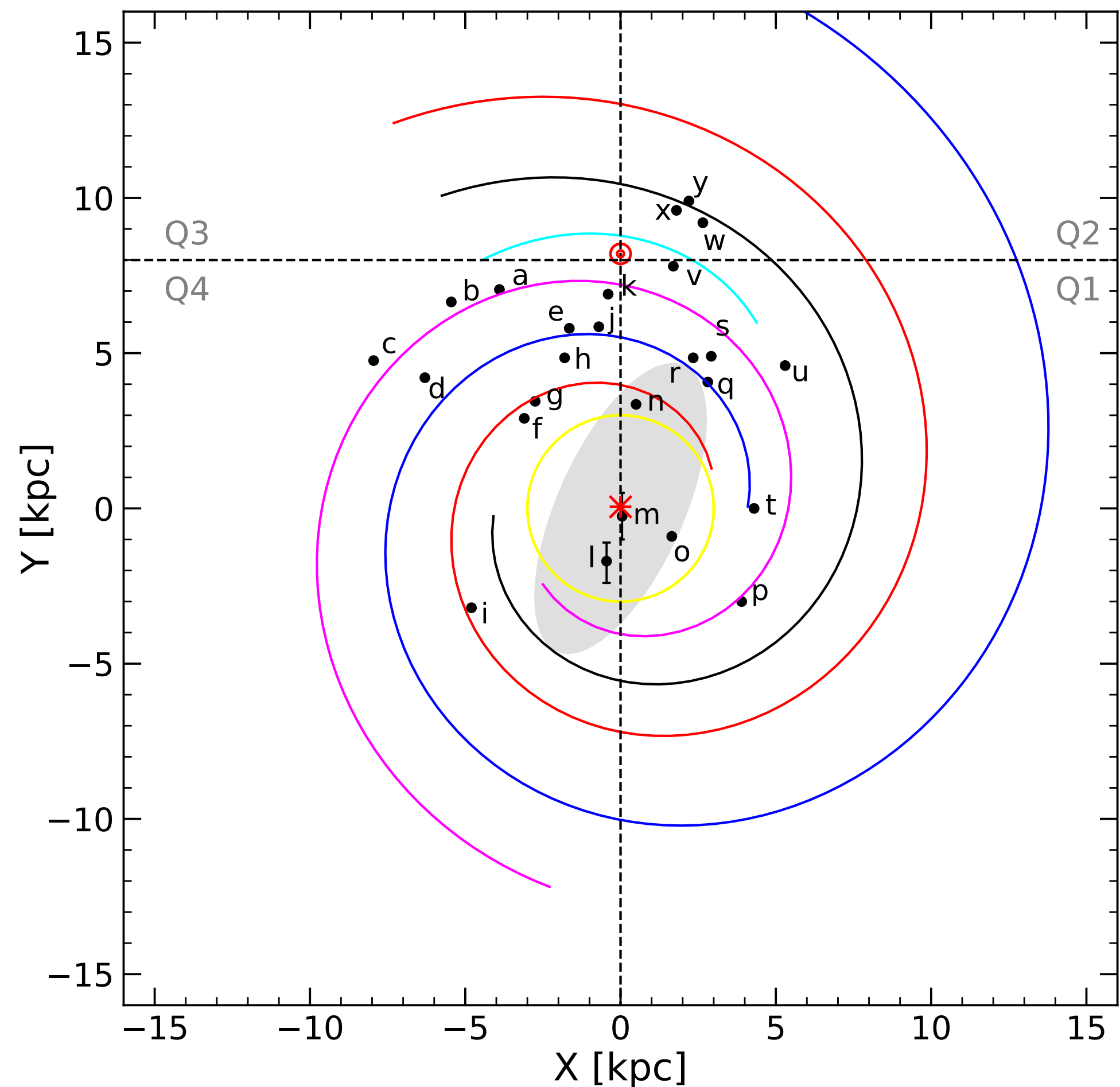
* Six hydrides (ArH⁺, H₂O⁺, OH⁺, SH, OH, and CH) and two atomic gas constituents (C⁺ and O)



✱ The SOFIA HyGAL observations were done with high-resolution setups using upGREAT (high-frequency array for OI and low-frequency array for CH and CII) and 4GREAT (for ArH⁺, H₂O⁺, OH⁺, SH, and OH).



Credit: Arshia Jacob

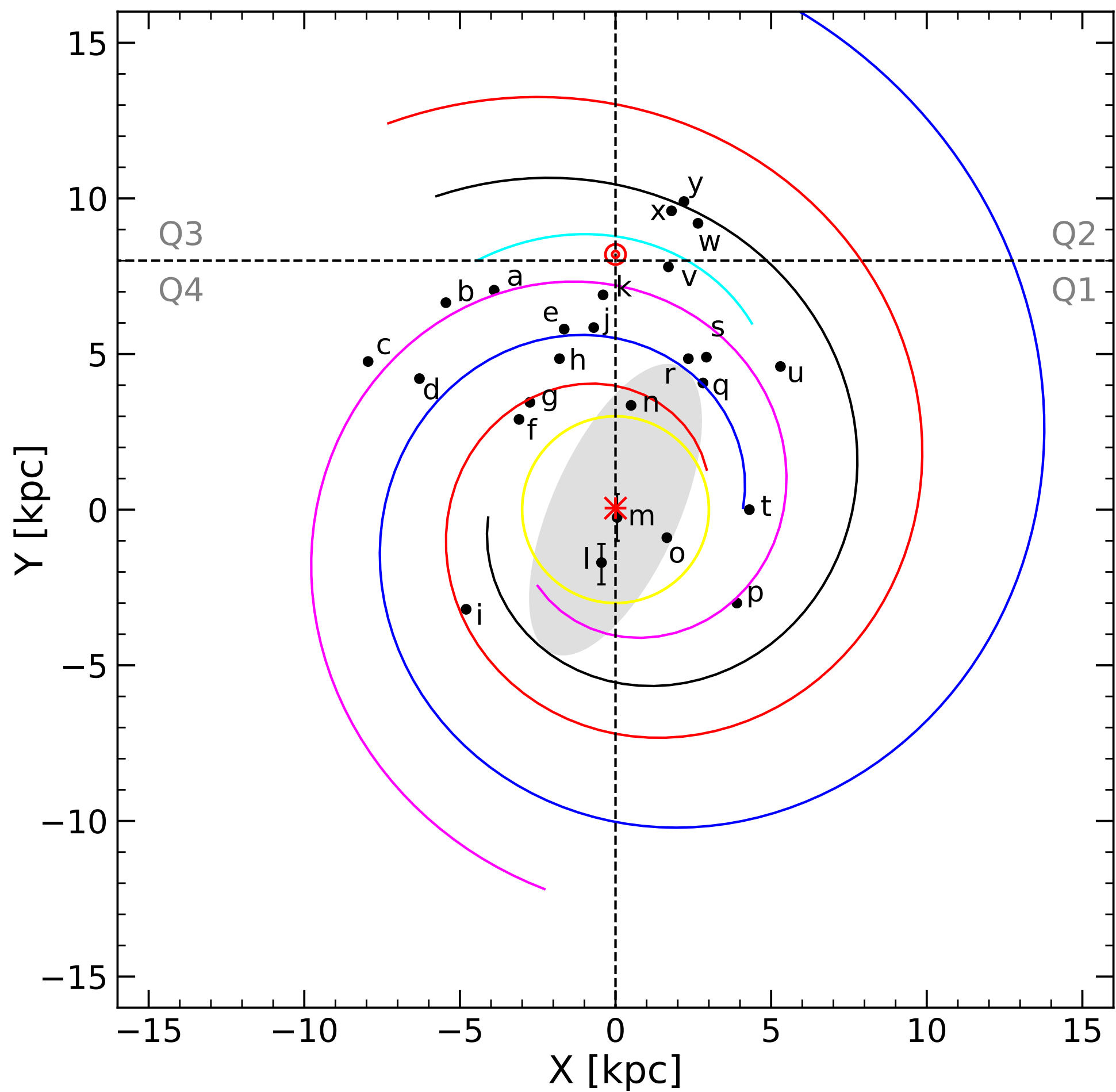


Distribution of HyGAL sources on the Galactic plane. Each latter corresponds to the sources listed in Table 1. Different colours indicate different spiral arms (Scutum- Centaurus arm, Local arm, 3-kpc arm, Norma and outer arms, Sagittarius- Carina arm , Perseus arm).

- Summary of HyGAL sources (HyGAL I; Overview paper, Jacob et al. 2022)

HyGAL Source Parameters								
#	Source Designation	R.A. (hh:mm:ss)	Decl. (dd:mm:ss)	Gal. Long. (deg)	Gal. Lat. (deg)	v_{LSR} (km s ⁻¹)	d [Ref] (kpc)	R_{GAL} (kpc)
a	HGAL284.015−00.86	10:20:16.1	−58:03:55.0	284.016	−0.857	9.0	5.7 [1]	9.0
b	HGAL285.26−00.05	10:31:29.5	−58:02:19.5	285.263	−0.051	3.4	4.3 [2]	8.2
c	G291.579−00.431	11:15:05.7	−61:09:40.8	291.579	−0.431	13.6	8.0 [3]	9.3
d	IRAS 12326-6245	12:35:35.9	−63:02:29.0	301.138	−0.225	−39.3	4.6 [4]	7.2
e	G327.3−00.60	15:53:05.0	−54:35:24.0	327.304	−0.551	−46.9	3.1 [5]	6.2
f	G328.307+0.423	15:54:07.2	−53:11:40.0	328.309	+0.429	−93.6	5.8 [6]	4.6
g	IRAS 16060−5146	16:09:52.4	−51:54:58.5	330.953	−0.182	−91.2	5.3 [7]	4.5
h	IRAS 16164−5046	16:20:11.9	−50:53:17.0	332.827	−0.551	−57.3	3.6 [8]	5.4
i	IRAS 16352−4721	16:38:50.6	−47:28:04.0	337.404	−0.403	−41.4	12.3 [4]	5.1
j	IRAS 16547−4247	16:58:17.2	−42:52:08.9	343.126	−0.063	−30.6	2.7 [8]	5.8
k	NGC 6334 I	17:20:53.4	−35:47:01.5	351.417	+0.645	−7.4	1.3 [9]	7.0
l	G357.558−00.321	17:40:57.2	−31:10:59.3	357.557	−0.321	5.3	9.0–11.8 [10]	1.0–3.6
m	HGAL0.55−0.85	17:50:14.5	−28:54:30.7	0.546	−0.851	16.7	7.7–9.2 [11]	0.4–1.0
n	G09.62+0.19	18:06:14.9	−20:31:37.0	9.620	+0.194	4.3	5.2 [12]	3.3
o	G10.47 + 0.03	18:08:38.4	−19:51:52.0	10.472	+0.026	67.6	8.6 [13]	1.6
p	G19.61−0.23	18:27:38.0	−11:56:39.5	19.608	−0.234	40.8	12.6 [14]	4.7
q	G29.96−0.02	18:46:03.7	−02:39:21.2	29.954	−0.016	97.2	6.7 [6]	4.5
r	G31.41+0.31	18:47:34.1	−01:12:49.0	31.411	+0.307	98.2	4.9 [15]	5.0
s	W43 MM1	18:47:47.0	−01:54:28.0	30.817	−0.057	97.8	5.5 [15]	5.0
t	G32.80+0.19	18:50:30.6	−00:02:00.0	32.796	+0.191	14.6	13.0 [16]	7.4
u	G45.07+0.13	19:13:22.0	+10:50:54.0	45.071	+0.133	59.2	4.3 [17]	6.2
v	DR21	20:39:01.6	+42:19:37.9	81.681	0.537	−4.0	1.5 [18]	7.4
w	NGC 7538 IRS1	23:13:45.3	+61:28:11.7	111.542	0.777	−59.0	2.6 [19]	9.8
x	W3 IRS5	02:25:40.5	+62:05:51.0	133.715	1.215	−39.0	2.3 [20]	9.9
y	W3(OH)	02:27:04.1	+61:52:22.1	133.948	1.064	−48.0	2.0 [20, 21]	9.6

- Continuum flux at 160 μm > 2000 Jy for inner Galactic sources
> 1000 Jy for outer Galactic sources
- These sources are selected from the Hi-GAL source catalog (Elia et al. 2021)



Distribution of HyGAL sources on the Galactic plane. Each latter corresponds to the sources listed in Table 1. Different colours indicate different spiral arms (Scutum- Centaurus arm, Local arm, 3-kpc arm, Norma and outer arms, Sagittarius-Carina arm , Perseus arm).

Summary of observation and detections of OH, CH, and OI (Kim et al. in prep)

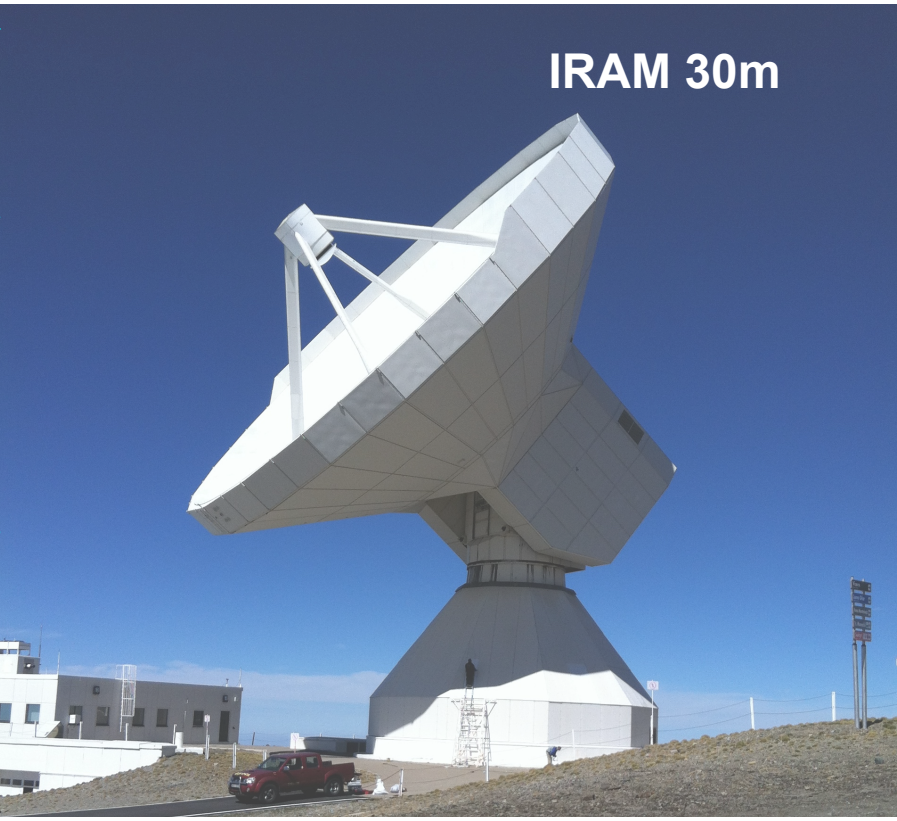
Source	OH				CH				OI			
	Flight	D	T _{cont}	T _{rms}	Flight	D	T _{cont}	T _{rms}	Flight	D	T _{cont}	T _{rms}
HGAL284.015−00.86	OC9S	x ^a	2.420	0.390	OC9S	− ^b	—	—	OC9S	x	2.000	0.228
HGAL285.26−00.05	OC9S	− ^b	—	—	OC9S	− ^b	—	—	OC9S	x	2.390	0.406
G291.579−00.431	OC9S	x	3.140	0.318	OC9S	− ^b	—	—	OC9S	x	0.766	0.252
IRAS 12326-6245	OC9S	− ^b	—	—	OC9S	− ^b	—	—	OC9S	x	2.740	0.325
G327.3−00.60	(1)	x	3.600	0.154	(2)	x	2.502	0.021	(2)	x	0.354	0.031
G328.307+0.423	OC9S	x	5.080	0.295	OC9S	− ^b	—	—	OC9S	x	2.460	0.216
IRAS 16060−5146	OC9BC	x	10.934	0.028	(3)	x	11.836	0.021	OC9BC	x	2.170	0.079
IRAS 16164−5046	OC9BC	x	9.850	0.218	(1)	x	7.759	0.066	OC9BC	x	3.140	0.213
IRAS 16352−4721	OC9S	x ^a	6.610	0.096	OC9S	− ^b	—	—	OC9S	x	1.770	0.177
IRAS 16547−4247	OC9S	x	5.170	0.351	OC9S	− ^b	—	—	OC9S	x	1.980	0.183
NGC 6334 I	OC9BC	x	17.332	0.418	OC9BC	x	15.297	0.076	OC9BC	x	9.000	0.104
G357.558−00.321	OC9S	− ^b	—	—	OC9N	x	1.575	0.072	OC9N,OC9S	x	0.627	0.07
HGAL0.55−0.85	OC9S	− ^b	—	—	OC9N	x	4.221	0.084	OC9N,OC9S	x	2.238	0.101
G09.62+0.19	OC9S	− ^b	—	—	OC9N	x	3.333	0.060	OC9N	x	1.000	0.099
G10.47+0.03	OC9S, (1)	x	6.900*	0.280*	(3)				OC9BC,OC9S	x	1.750	0.069
G19.61−0.23	OC9S	− ^b	—	—	OC9N	x	2.844	0.070	OC9N,OC9S	x	1.104	0.068
G29.96−0.02	OC9BC	x	5.700	0.536	OC9BC	x	3.571	0.049	OC9BC	x	4.950	0.681
G31.41+0.31	OC9S	x	1.860	0.338	OC9S	− ^b	—	—	OC9S	x	0.040	0.180
W43 MM1	OC9F	x	2.410	0.399	OC9F	x	2.110	0.101	OC9F	NO	0.650	1.137
G32.80+0.19	OC9BC	x	4.050	0.344	OC9BC	x	3.780	0.073	OC9BC	x	2.560	0.226
G45.07+0.13	OC9BC	x	5.310	0.313	OC9BC	x	2.983	0.065	OC9BC	x	3.650	0.508
DR21	OC9F	x	2.690	0.508	OC8H	x	1.727	0.063	OC8H,OC9F	x	0.730	0.086
NGC 7538 IRS1	OC8H	x	4.420	0.423	OC8H	x	3.260	0.056	OC8H	x	3.010	0.051
W3 IRS5	OC8H,OC9F	x	8.610	0.392	OC8H	x	5.480	0.061	OC8H,OC9F	x	6.870	0.062
W3(OH)	OC8H,OC9F	x	6.450	0.271	OC8H	x	5.300	0.113	OC8H,OC9F	x	1.810	0.055

Notes. (1) Wiesemeyer et al. (2016) (2) Jacob et al. (2019) (3) Jacob et al. (2020). (a): Observations done with 50-60% observing time. (b): no observing time was allocated. For G10.47+0.03, OH data from Wiesemeyer et al. (2016) is used for this study because the data taken during the SOFIA flight is severely affected by atmosphere variations over the observations causing its poor baseline and abnormal absorption features.

Table 2. Summary of HyGAL observations

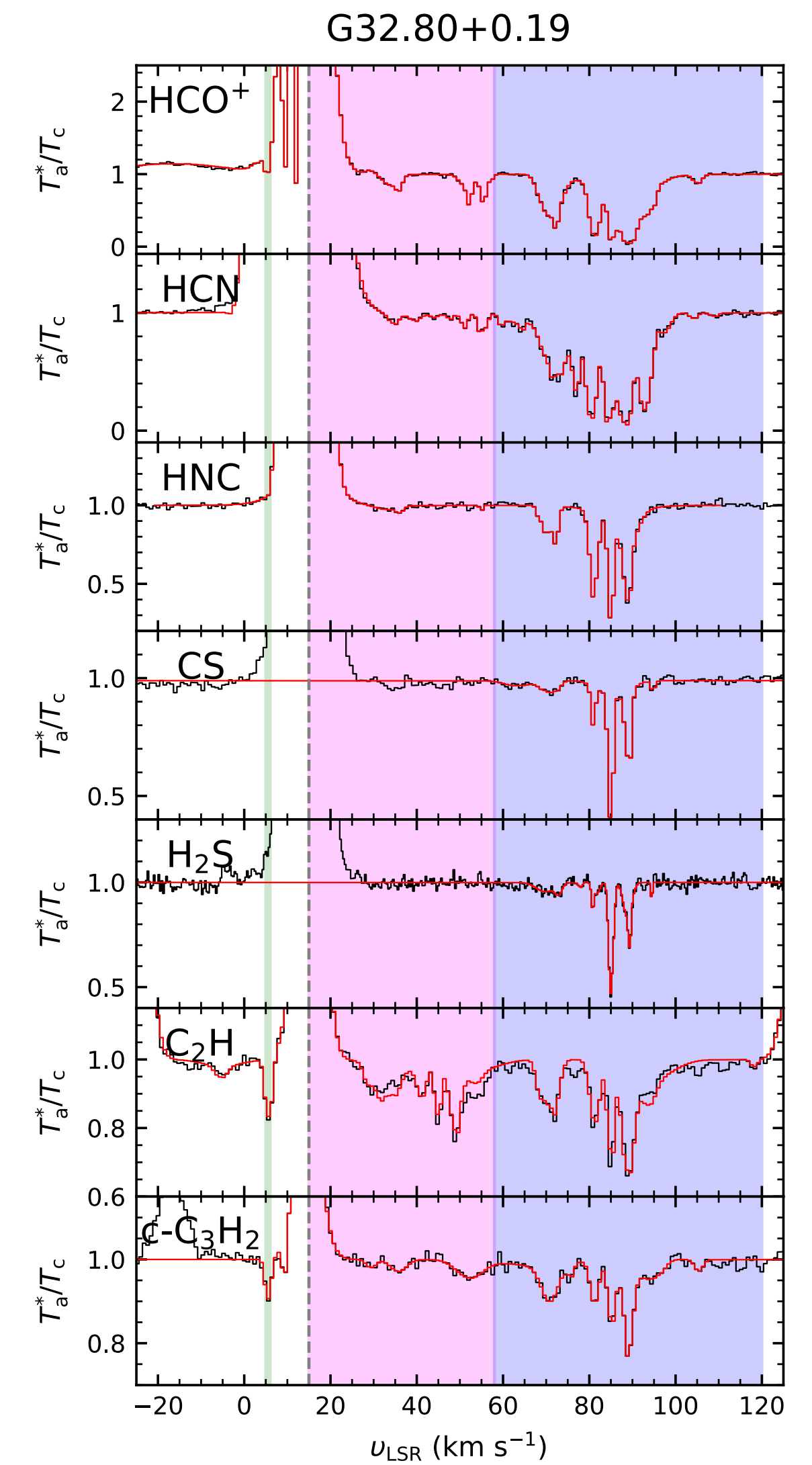
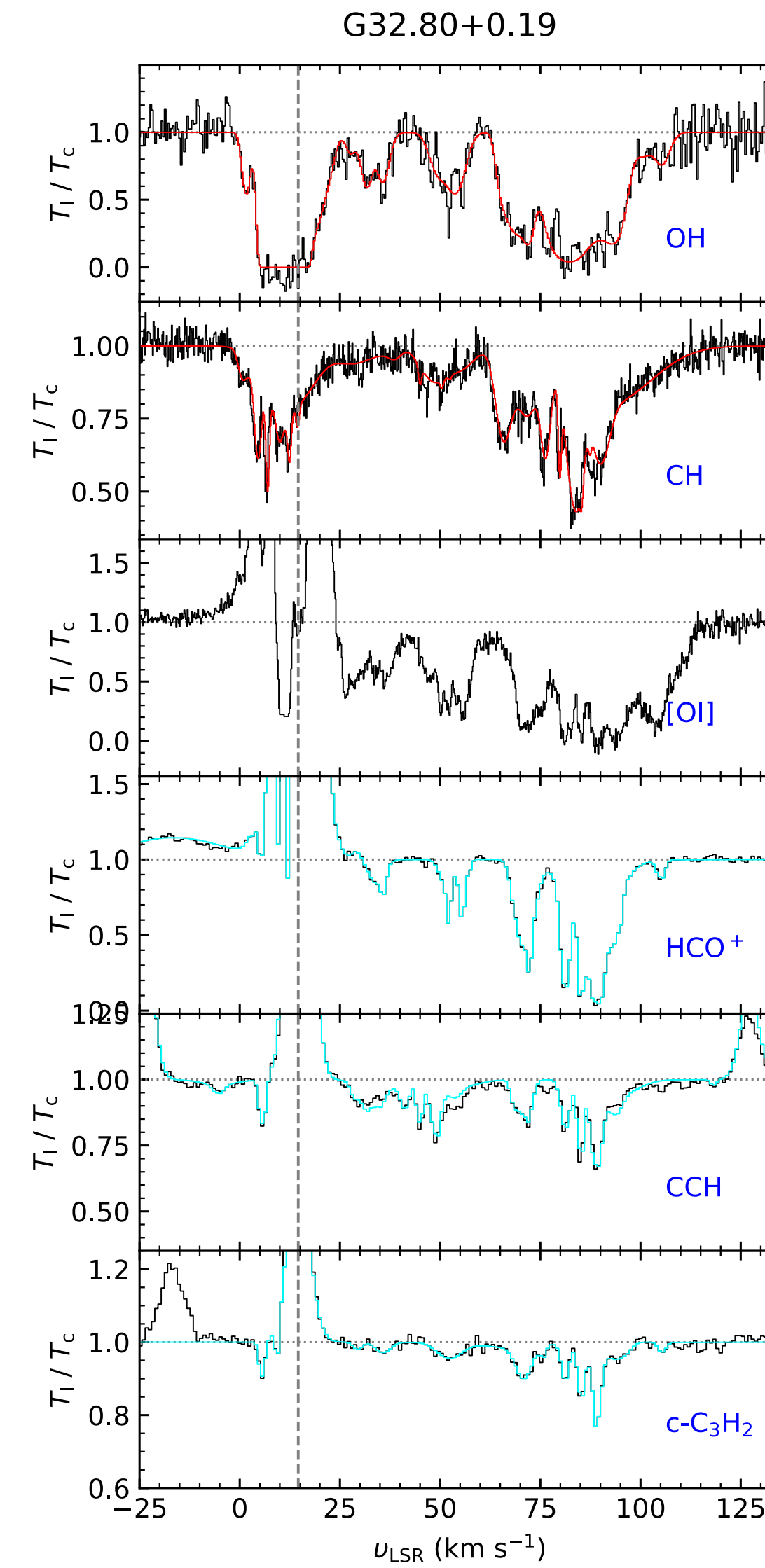
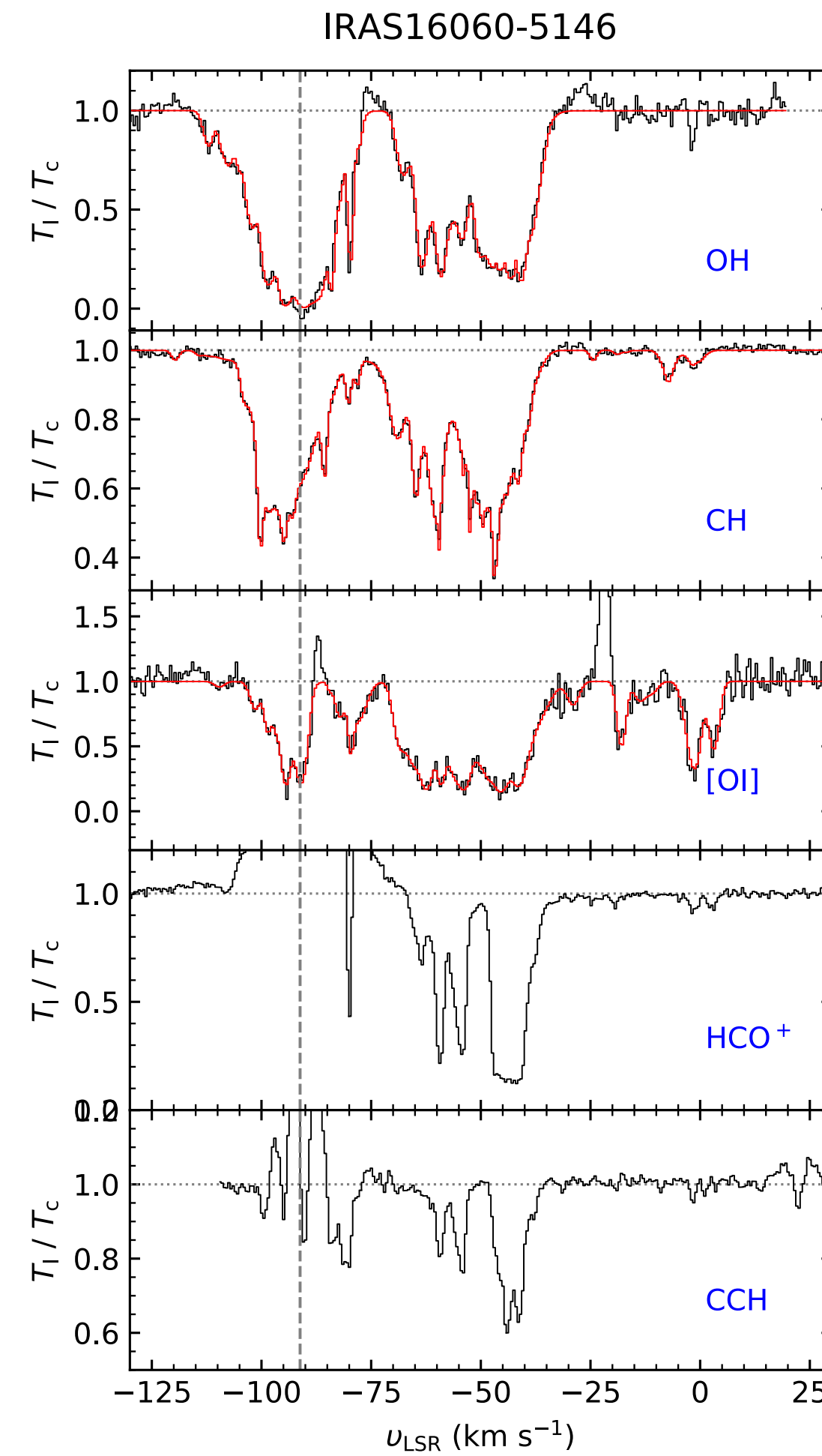
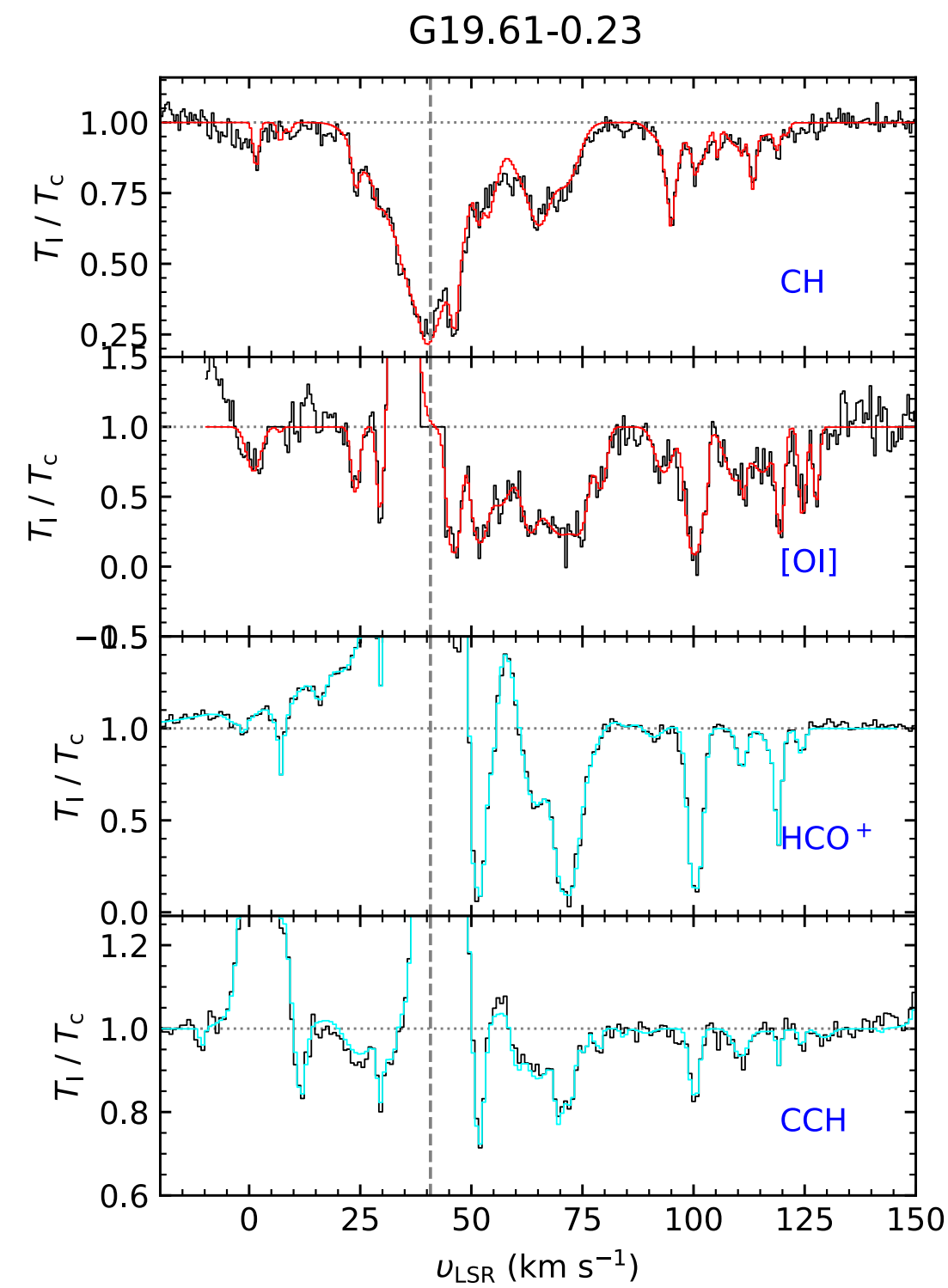
Telescope	SOFIA	IRAM 30 m *	NOEMA
Target species	ArH ⁺ , H ₂ O ⁺ , OH ⁺ , SH, OH, CH, C ⁺ , O	HCO ⁺ , HCN, HNC, CS, H ₂ S, C ₂ H, c-C ₃ H ₂	CO (12CO, 13CO, C18O, C17O), CN, CS#
Observed sources	25	15	9

Note) OH, CH, & O - [Kim et al. in prep](#); ArH⁺, H₂O⁺, OH⁺ - [Jacob et al. in prep](#)
(*) The 30m data is published as the HyGAL II ([Kim et al. 2023](#)).
NOEMA data ([PI: Wonju Kim](#)) : CO & CN - [Kim et al. in prep](#).
SOFIA & NOEMA: SH & CS (#: also several isotopologues are observed) - [Jacob et al. in prep](#).



Real spectra in black and modelled spectra by XCLASS* in red

* the eXtended CASA Line Analysis Software Suite (XCLASS, Möller et al. 2017)



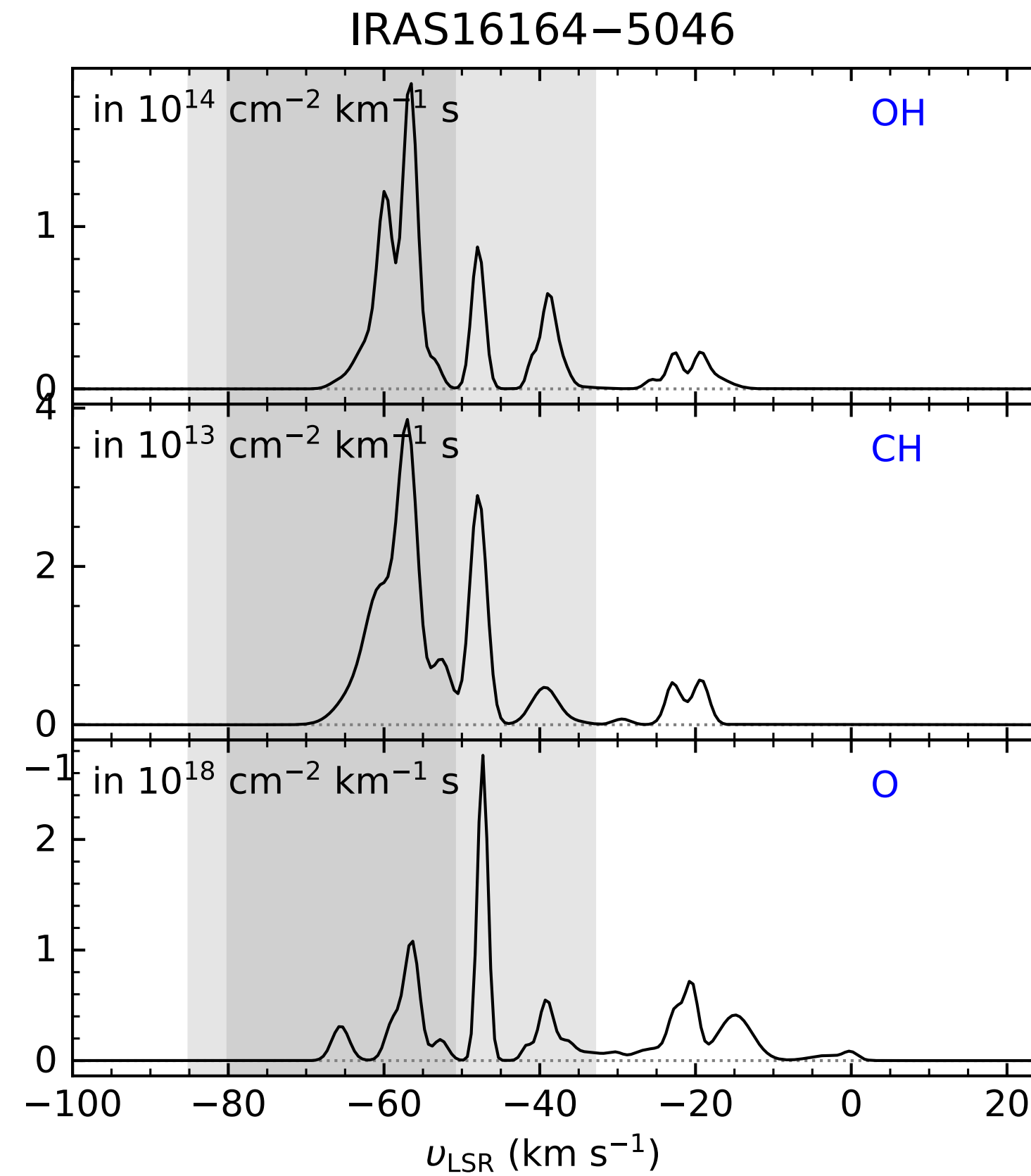
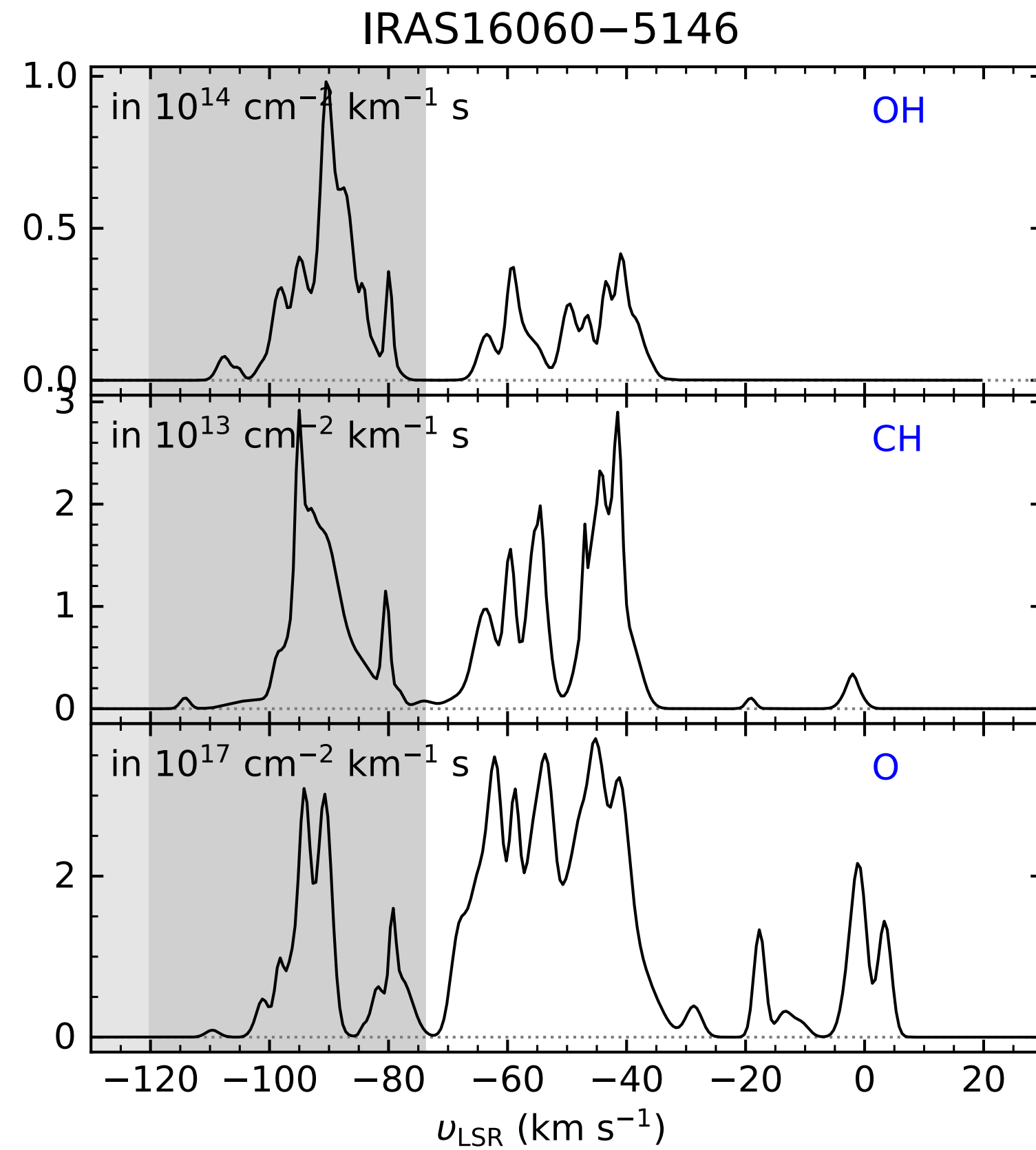
Aquila-Rift/Sagittarius-Carina arm/Scutum- Centaurus arm

(Kim et al. 2023)

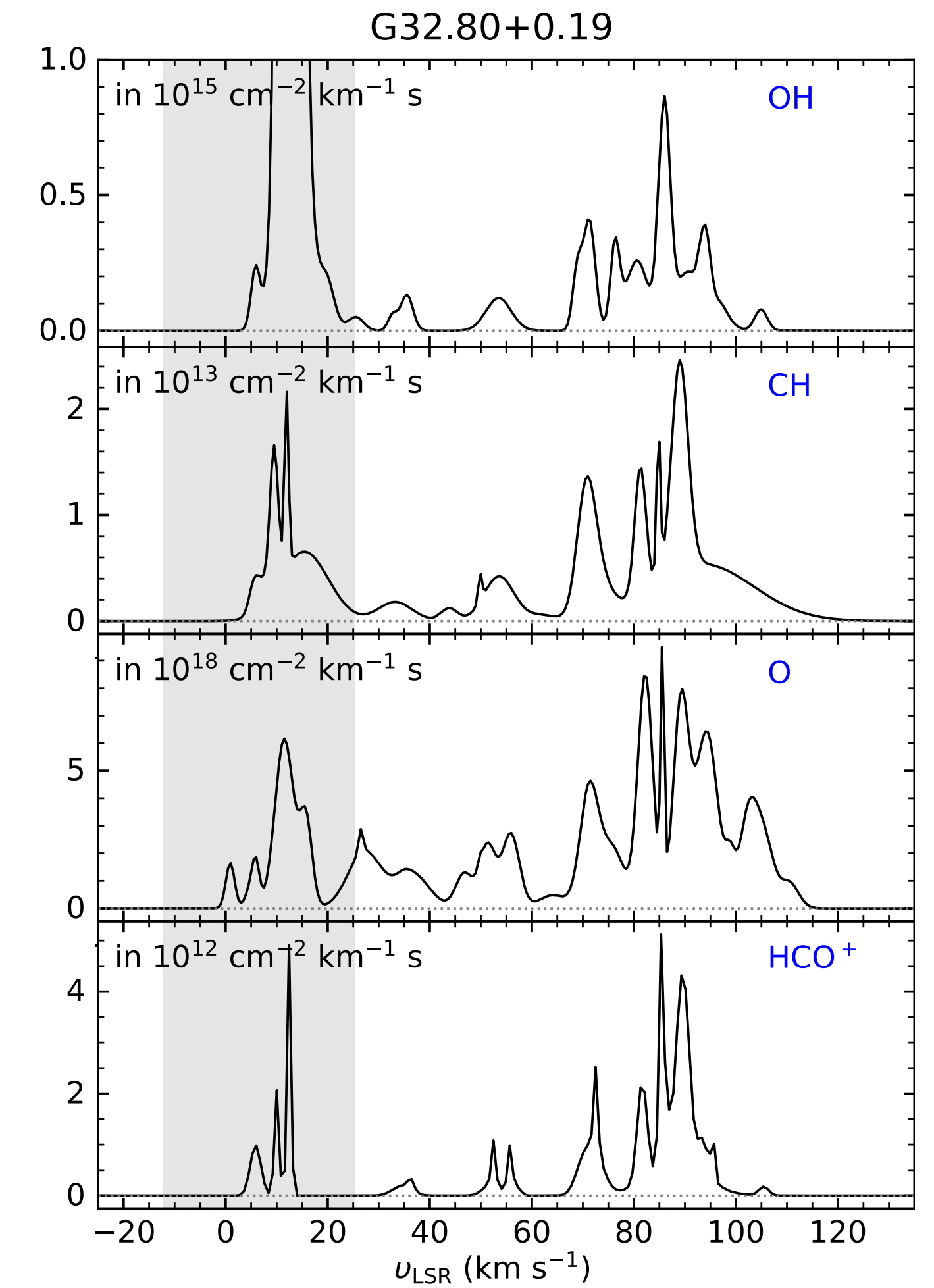
HyGAL:

Column density profiles of CH & OH

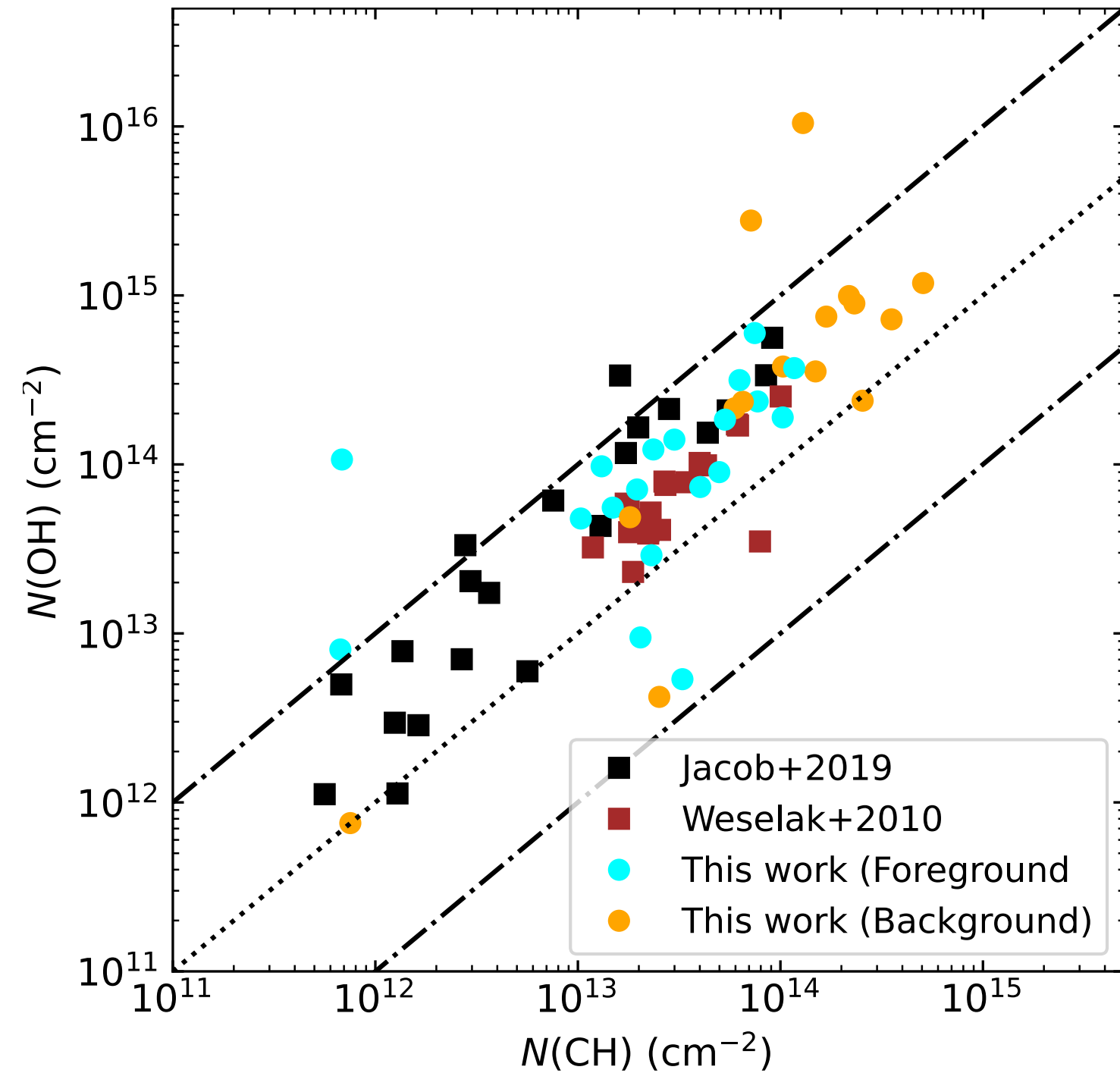
13



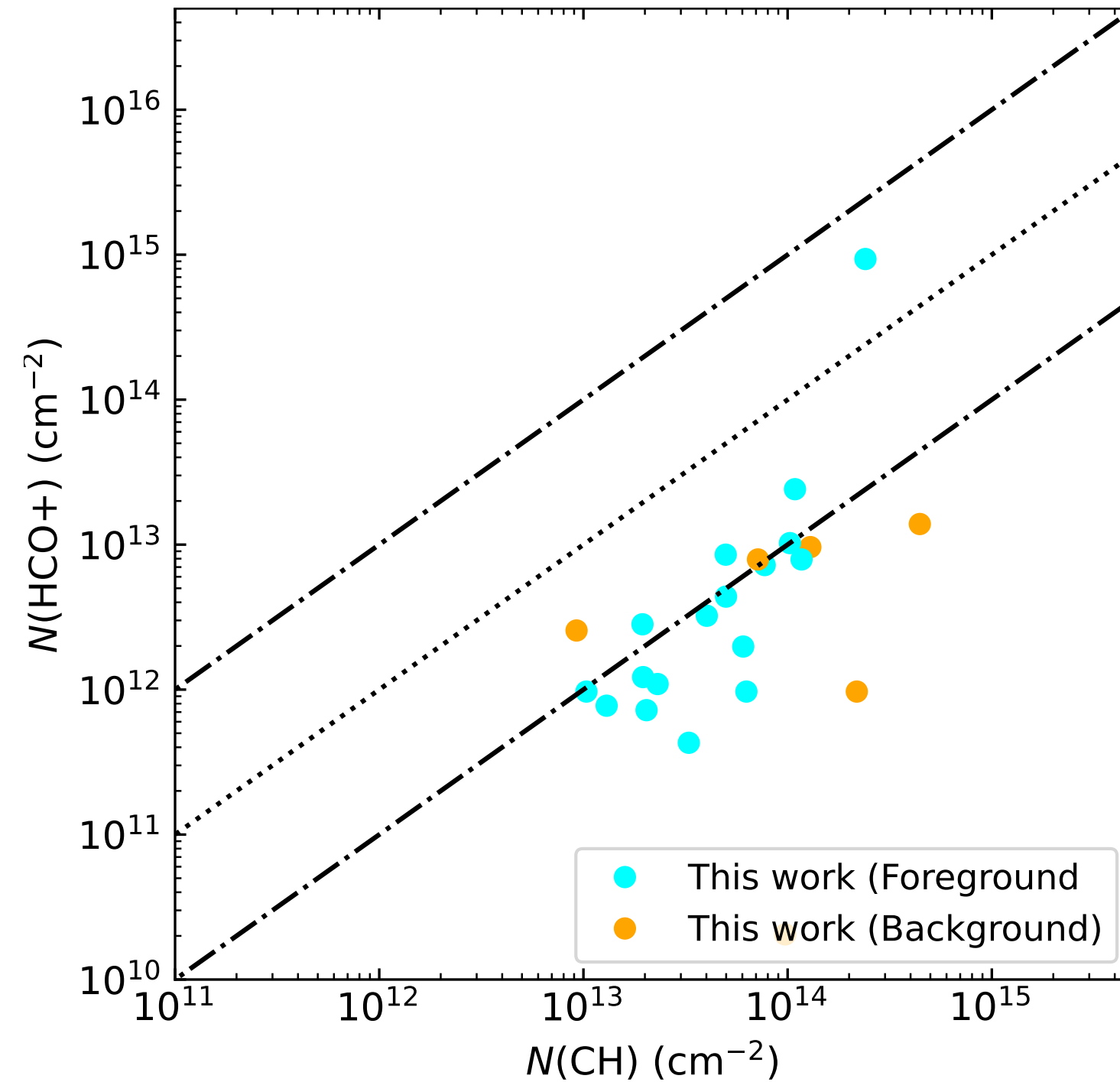
Velocity intervals of emission lines



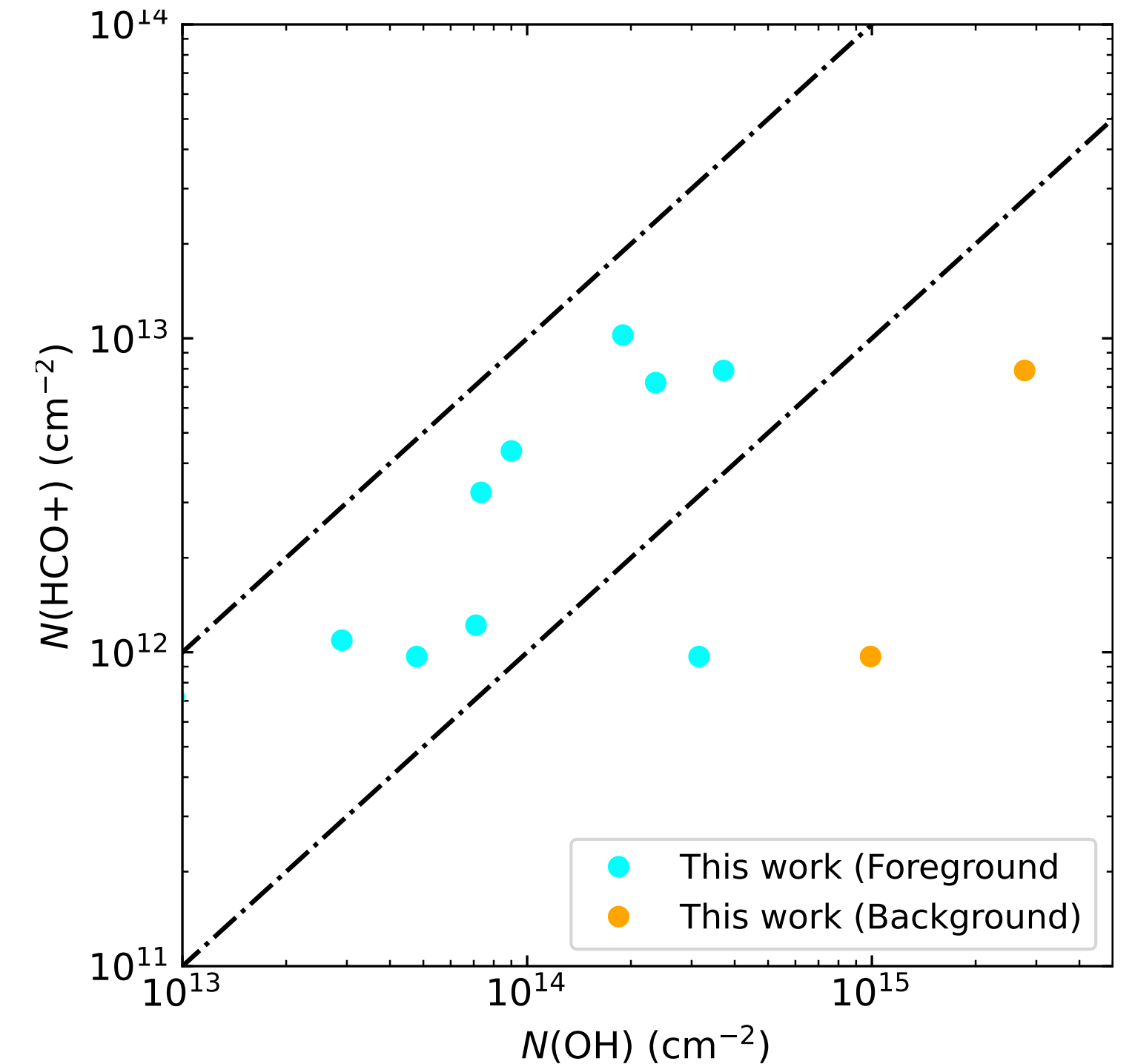
CH vs OH



CH vs HCO⁺

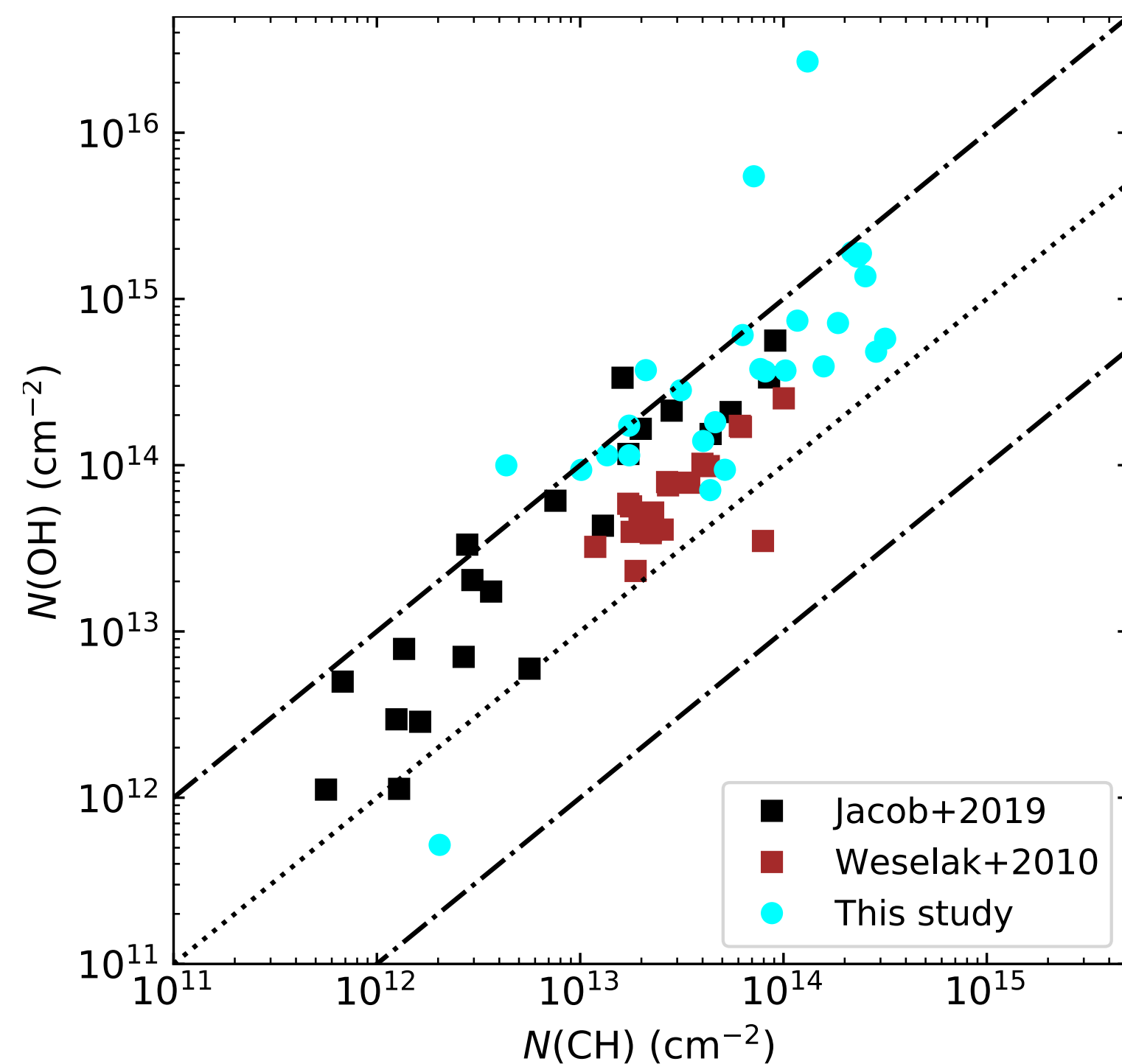


OH vs HCO⁺

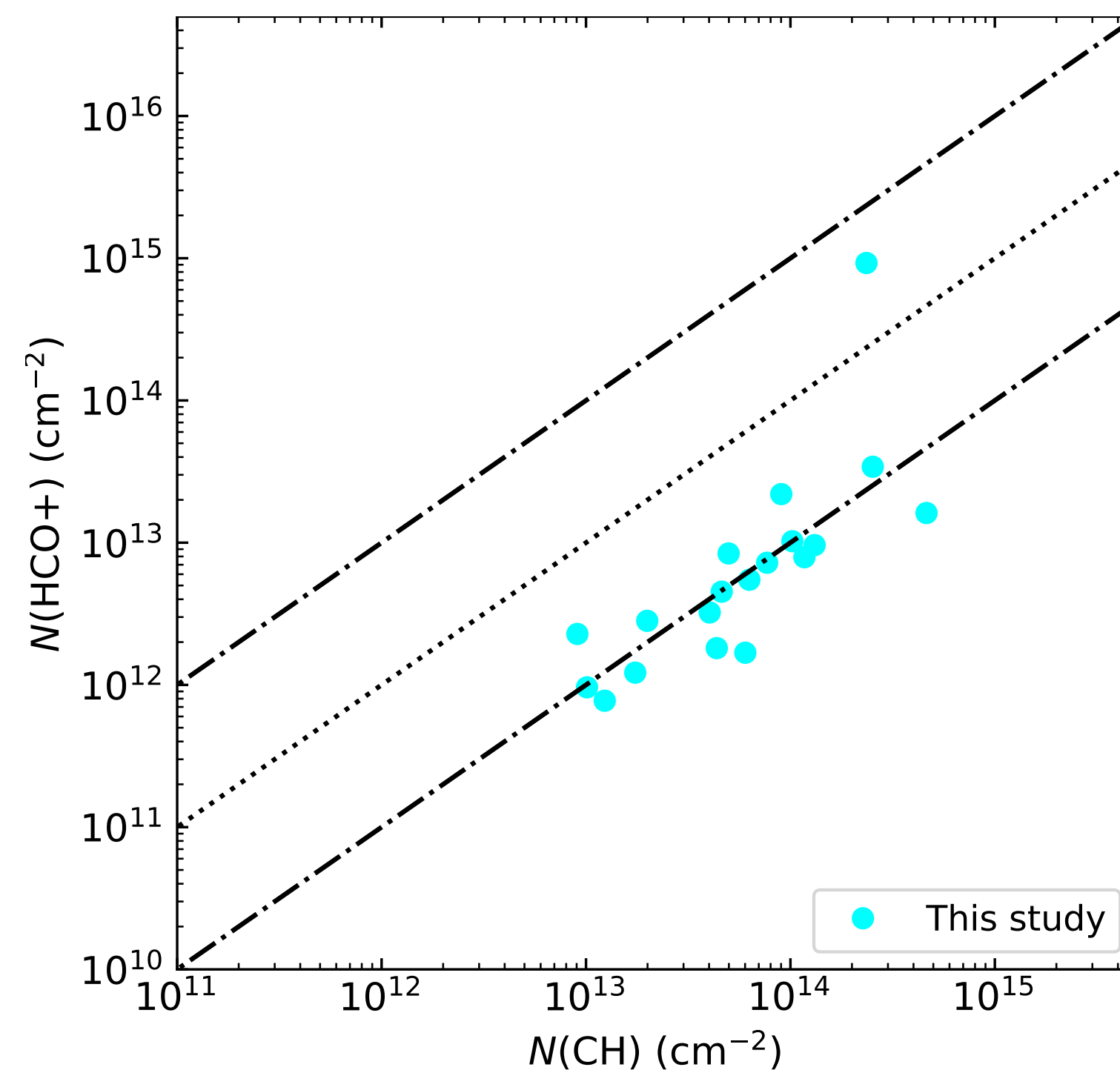


- CH and OH show a good correlation, but those species and HCO⁺ do not show such a strong linear-relationship.
- For these plots, velocity intervals are defined based on HI, OH, and OH⁺.
What if we define velocity ranges differently?

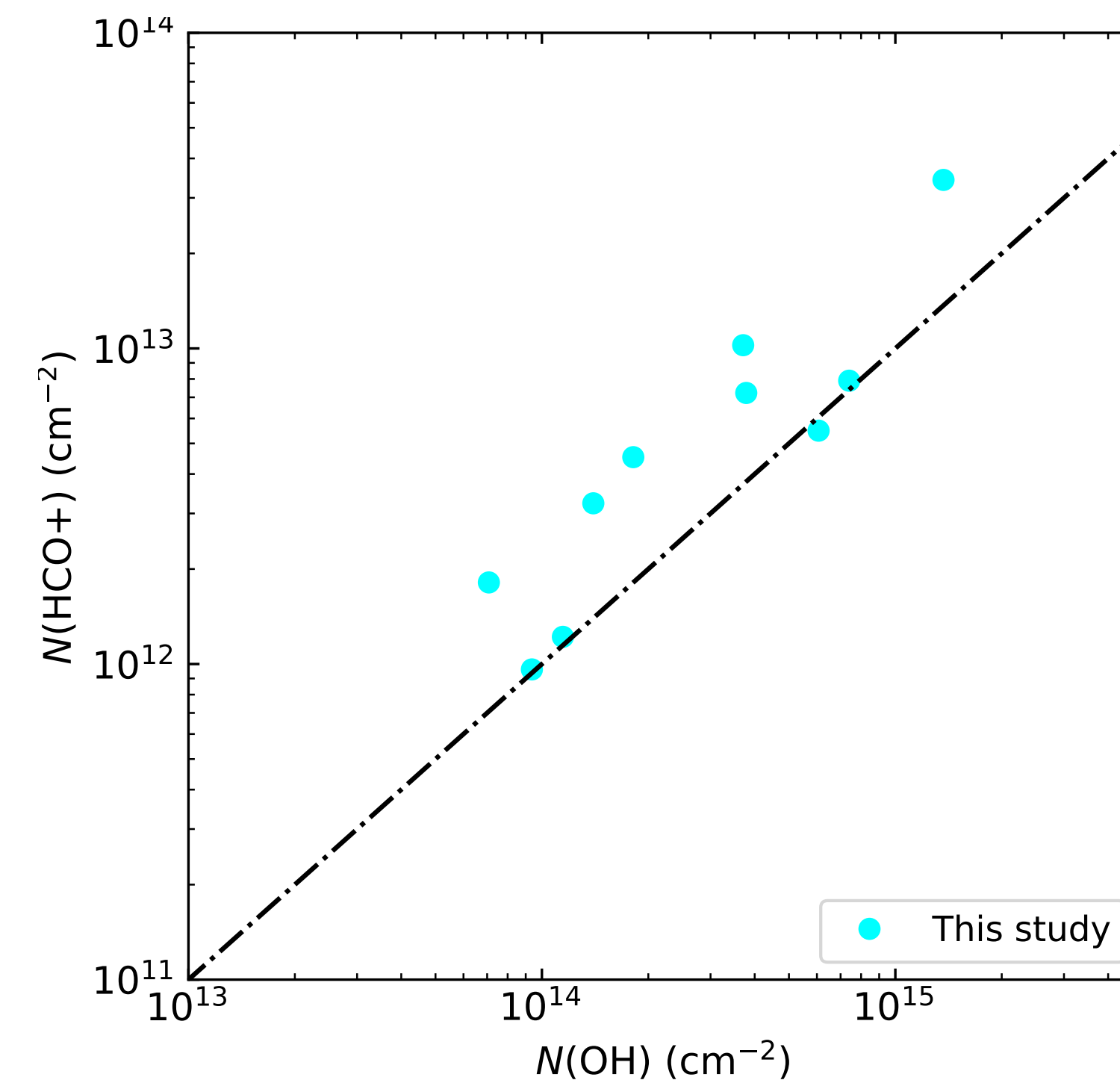
CH vs OH



CH vs HCO⁺

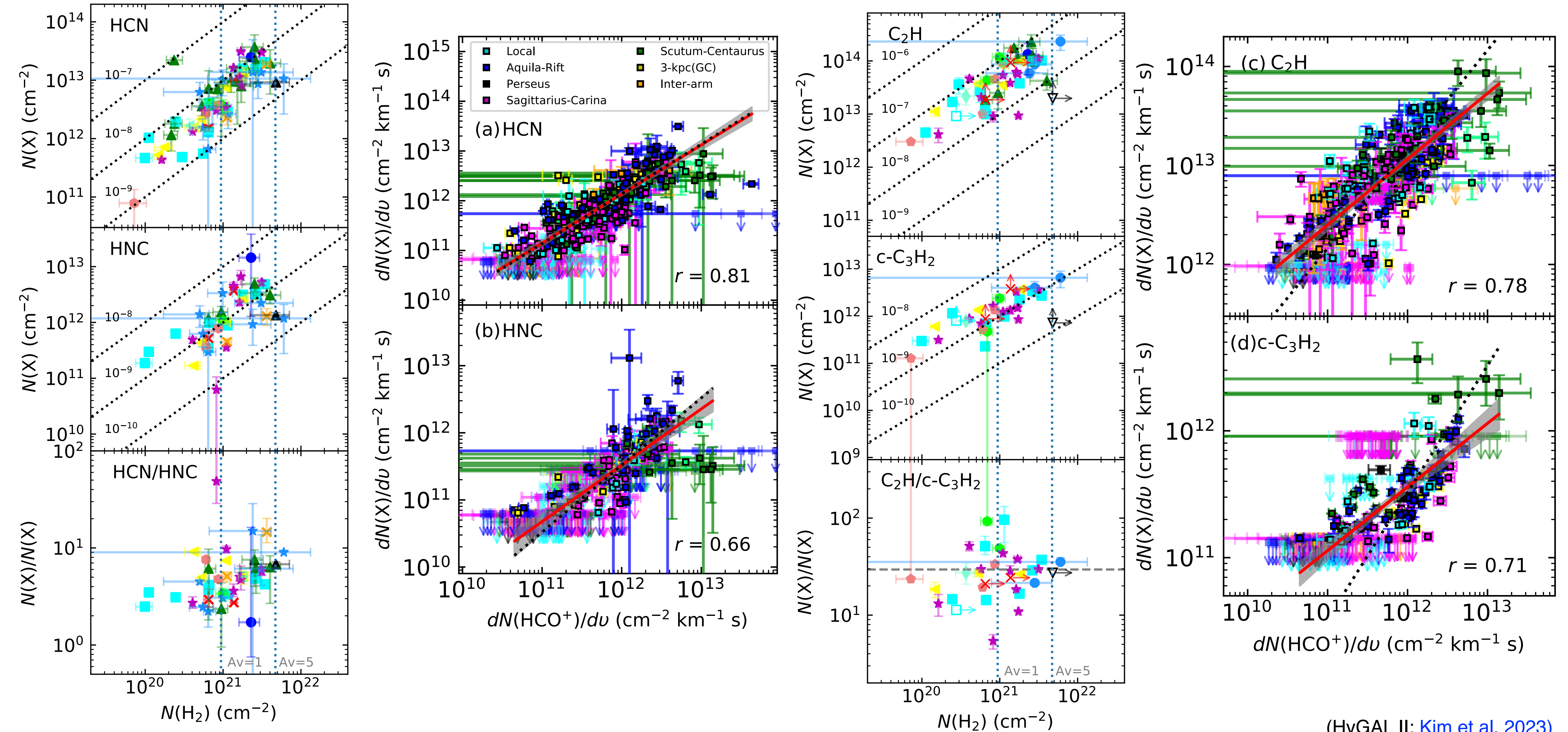


OH vs HCO⁺

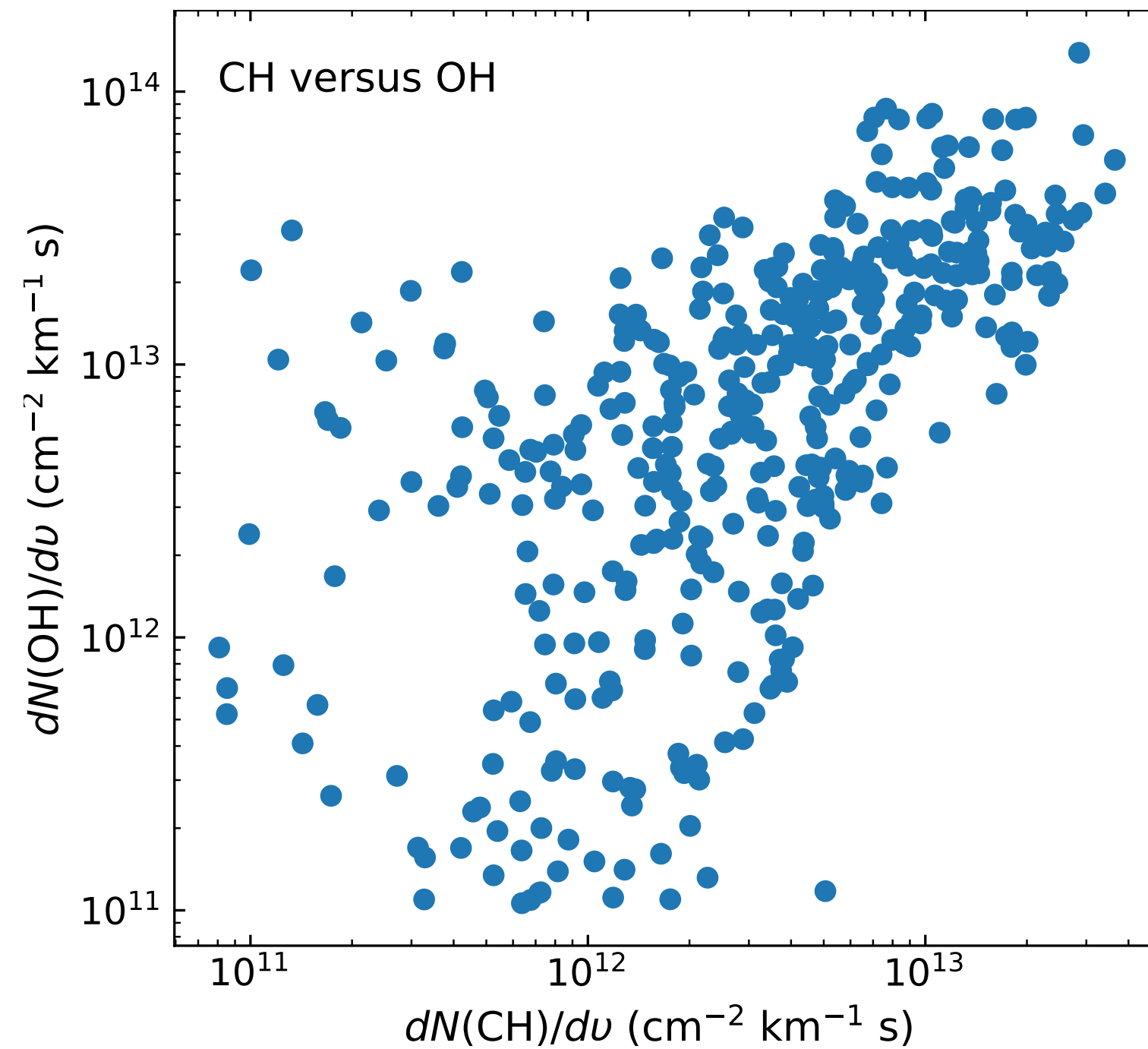


The velocity intervals are based on CH and OH column density profiles.

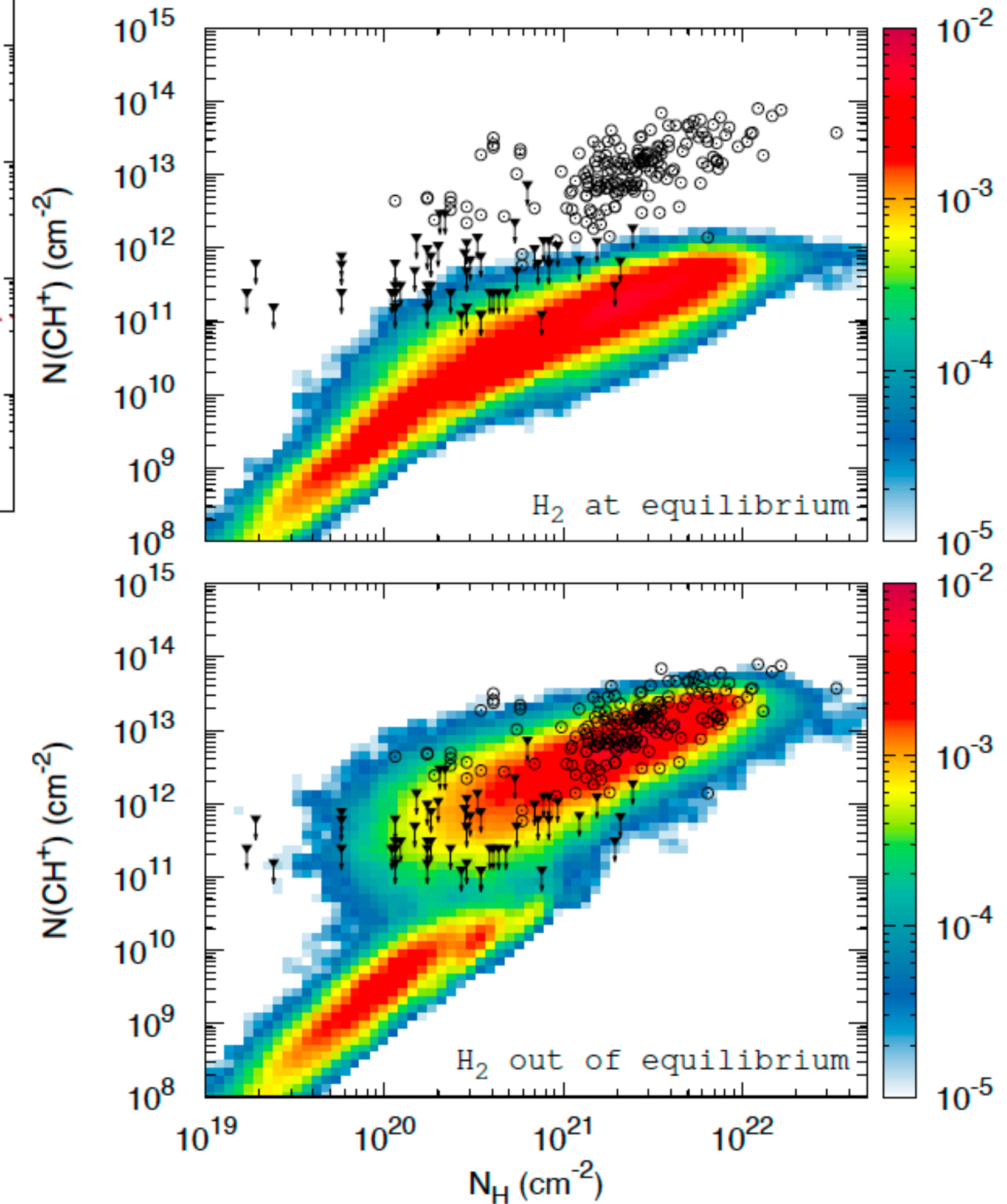
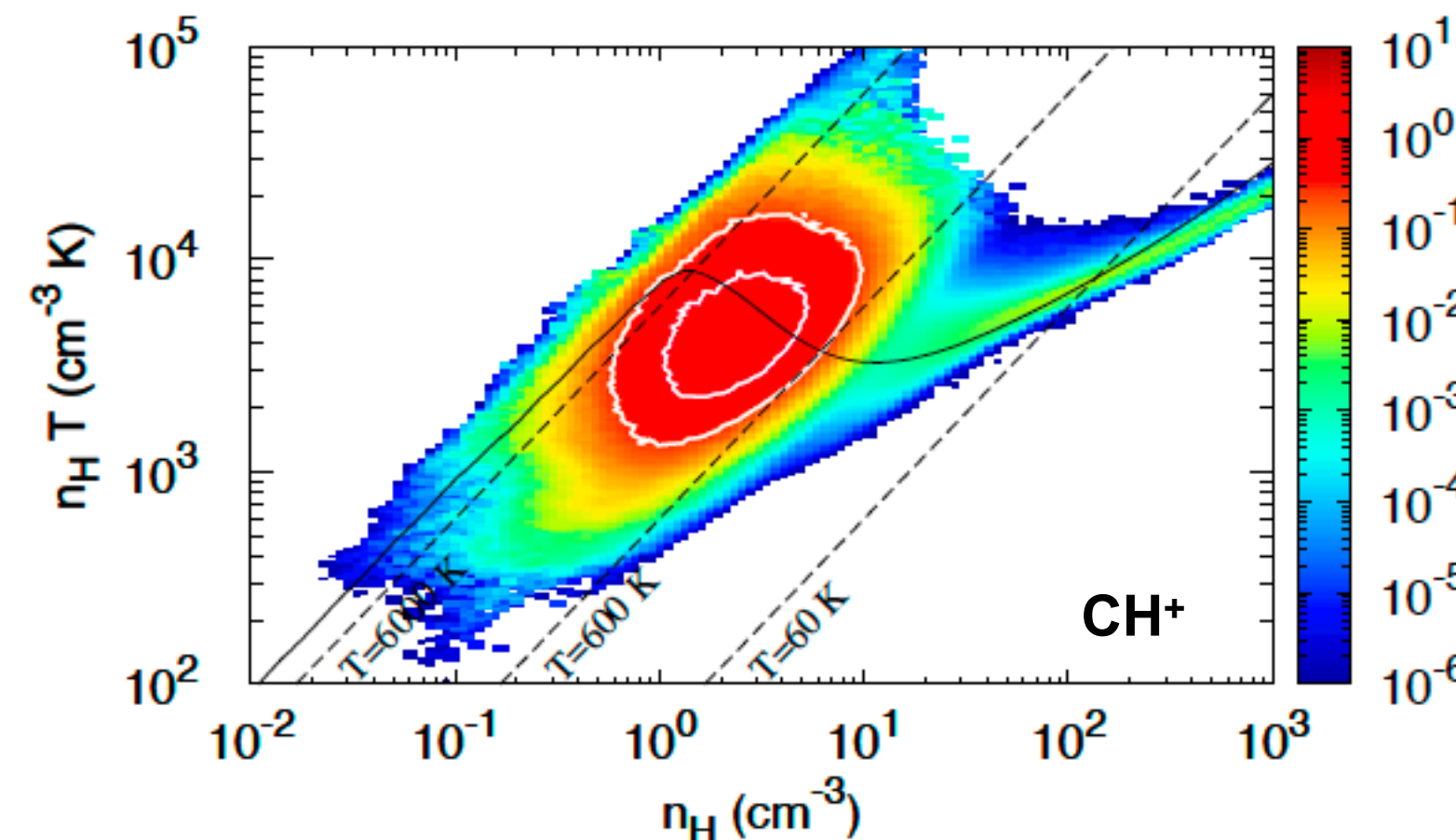
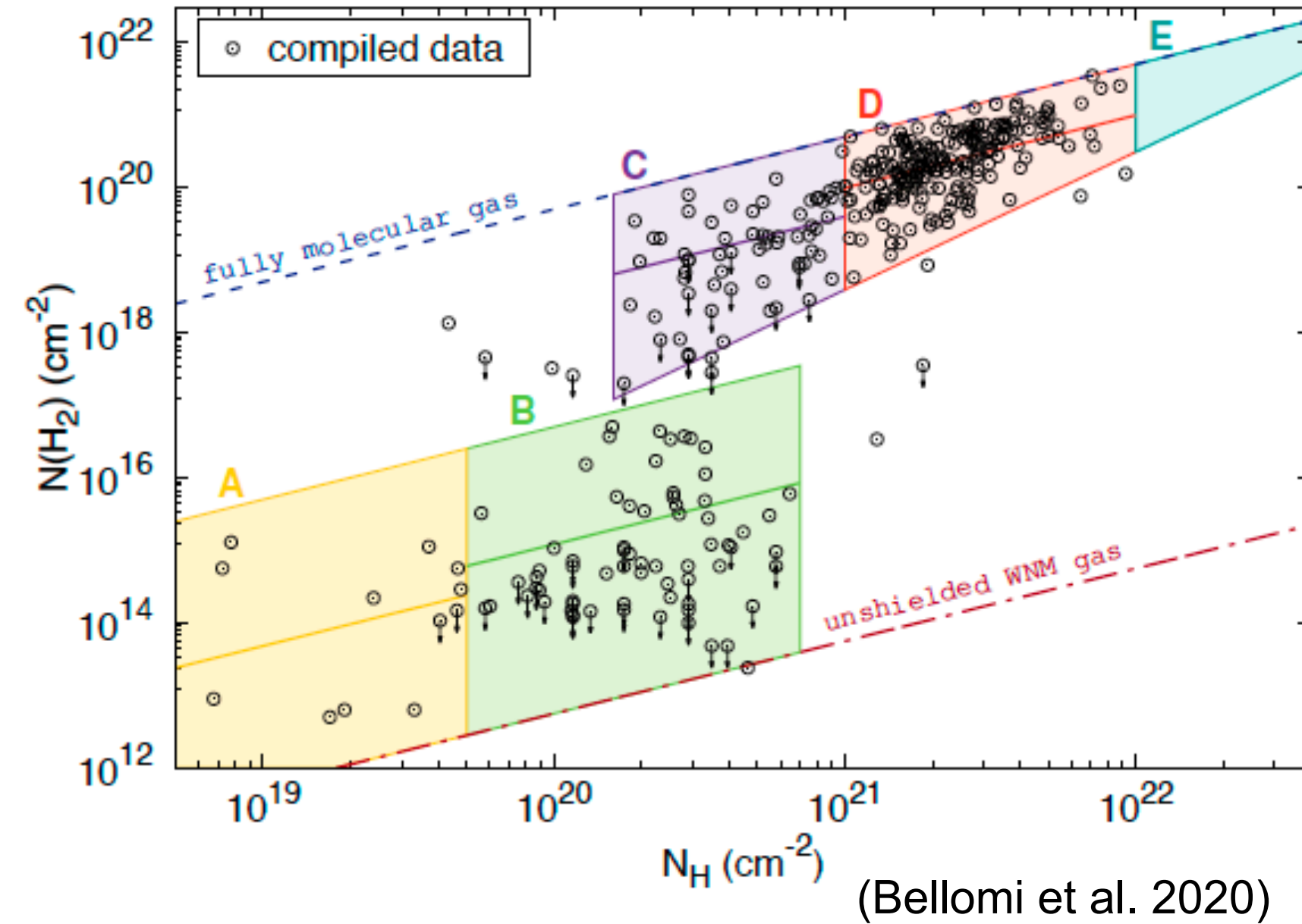
CH and OH now look having better correlation with HCO⁺!



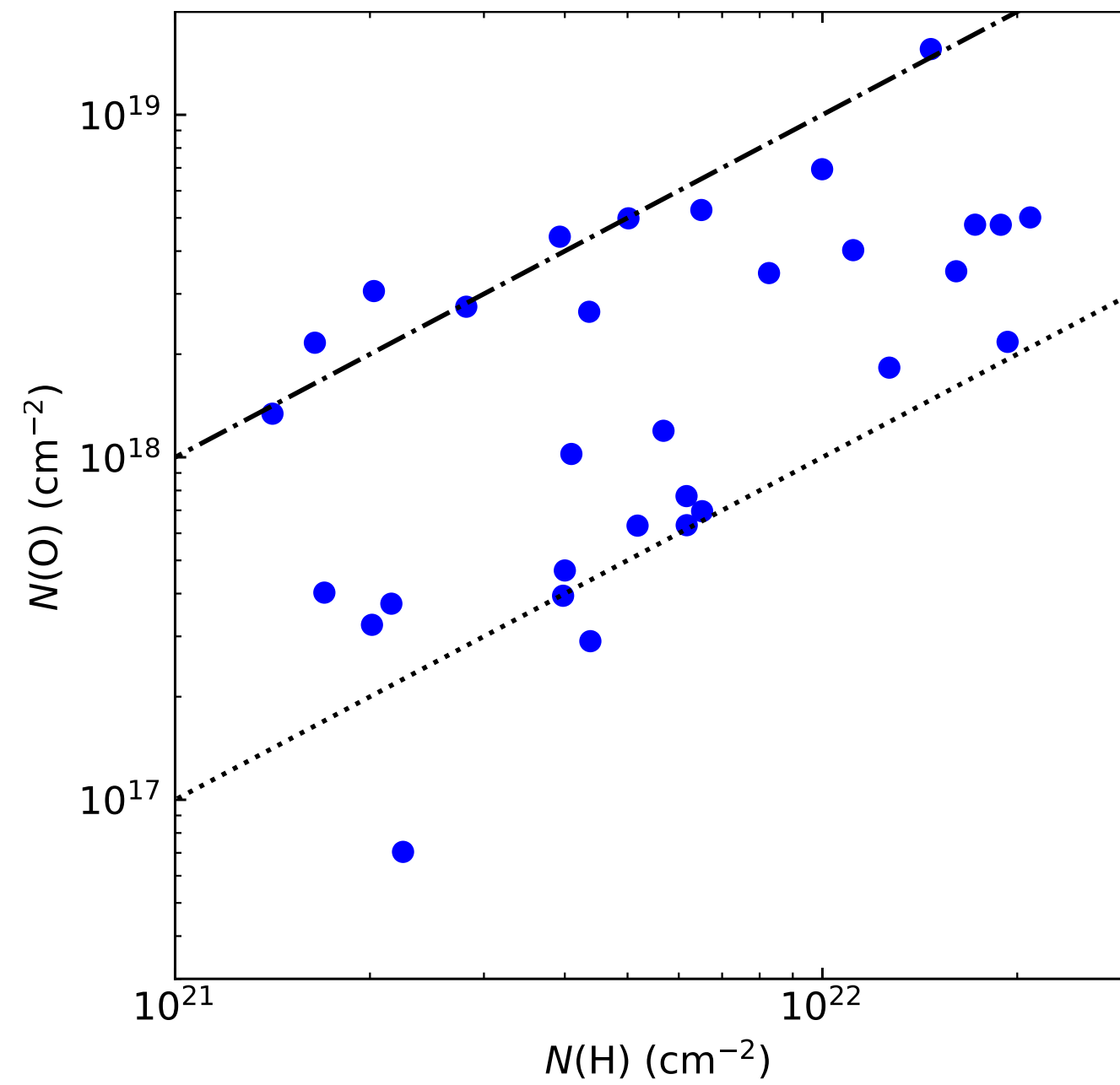
CH vs OH



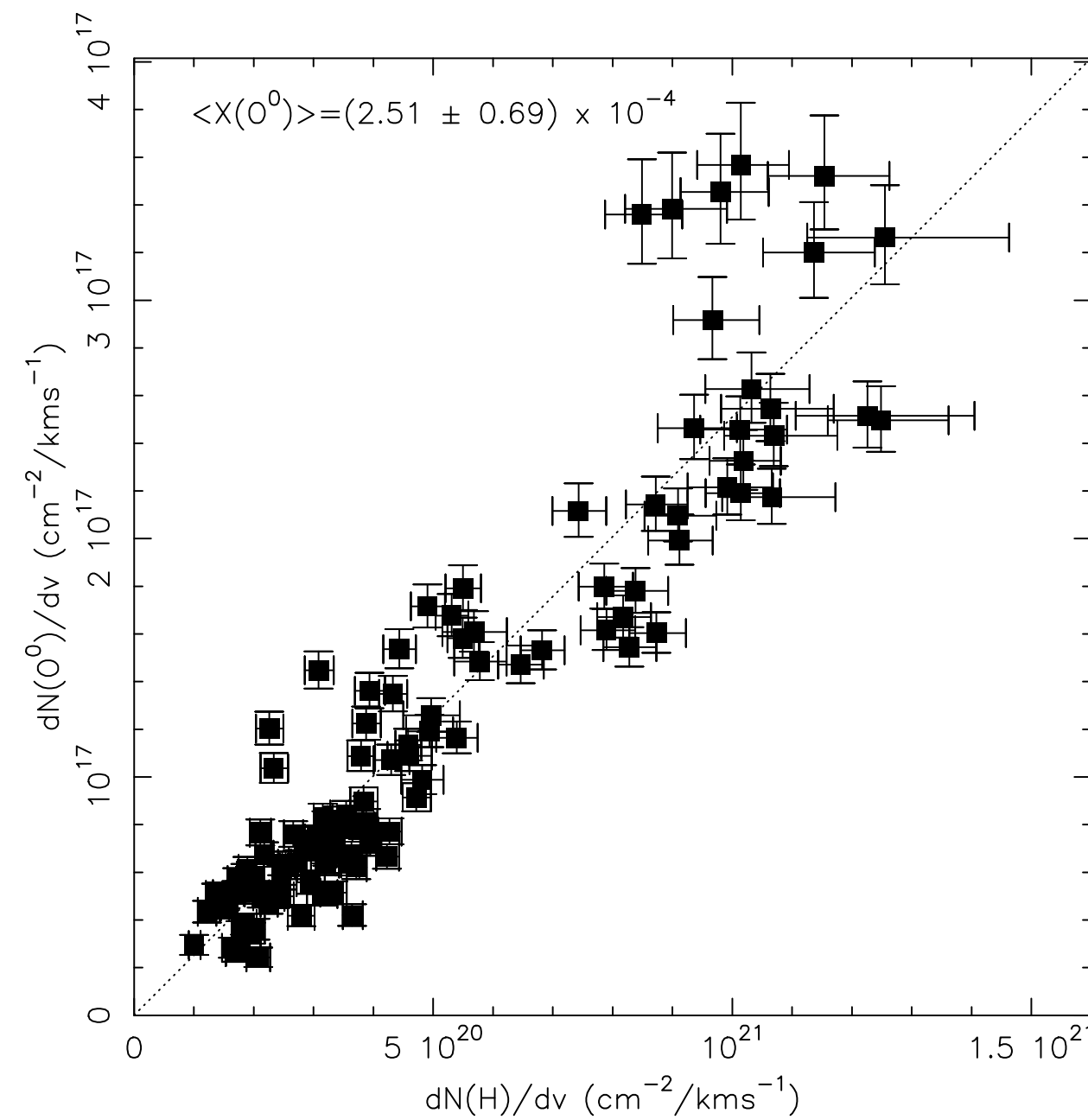
- These scatters could be related to diffuse molecular and translucent cloud components associated with multiple-phase mediums.



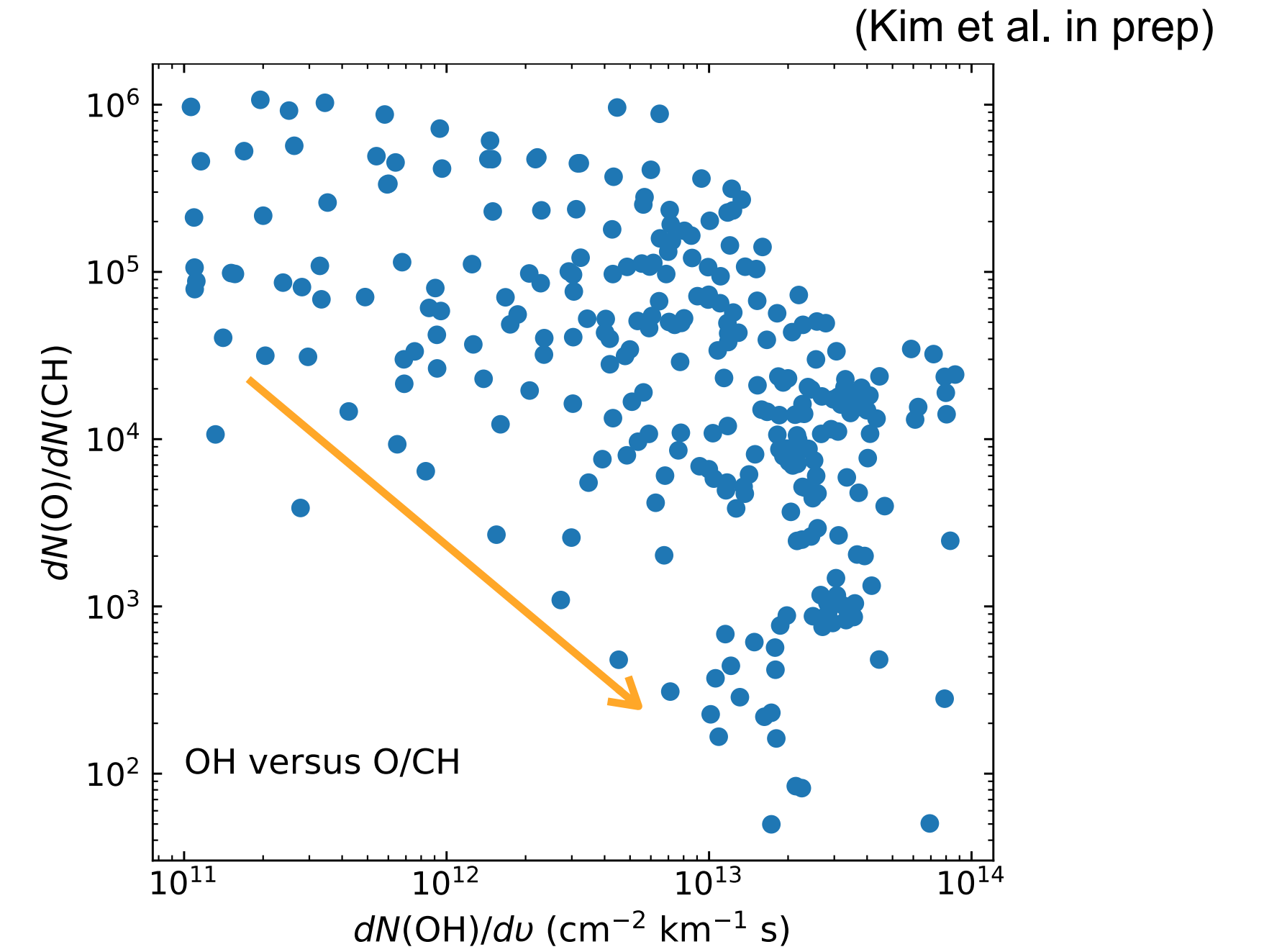
(Godard et al. 2023)



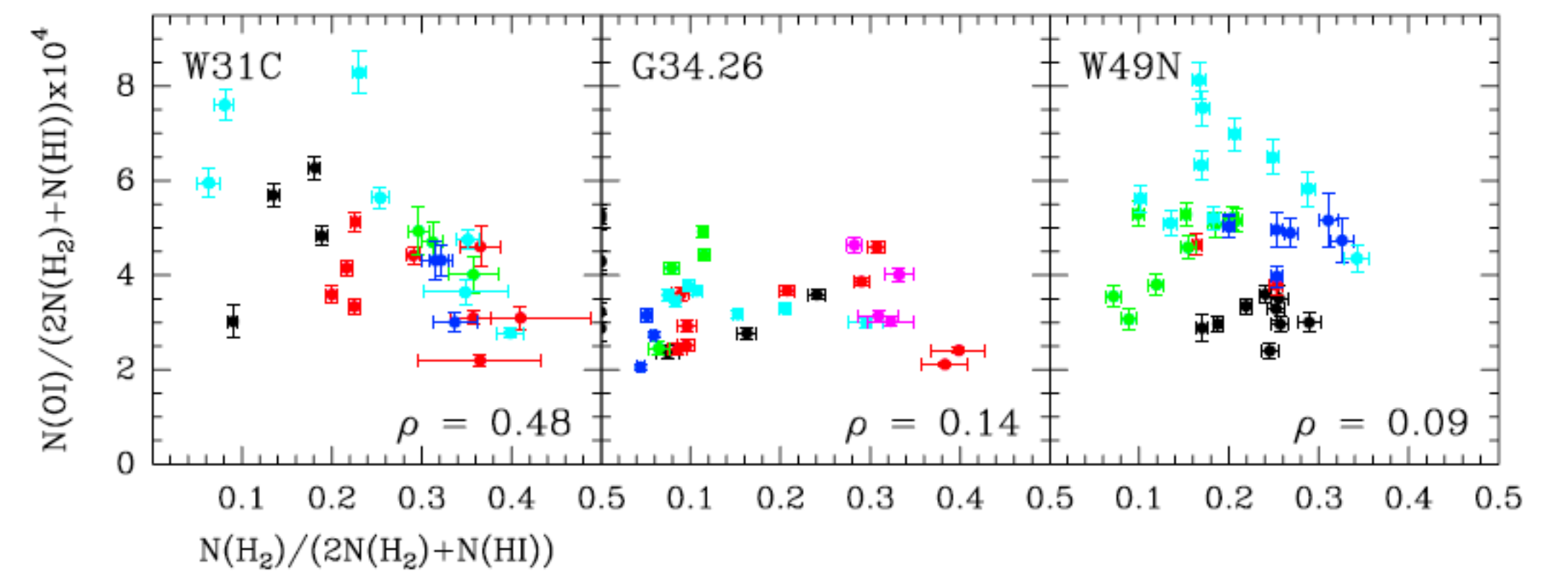
(Kim et al. in prep)



(Lis et al. 2023)



- There is some degree of scatters toward different lines of sight.
- Oxygens go to other oxygen-bearing species?



(Wiesemeyer et al. 2016)

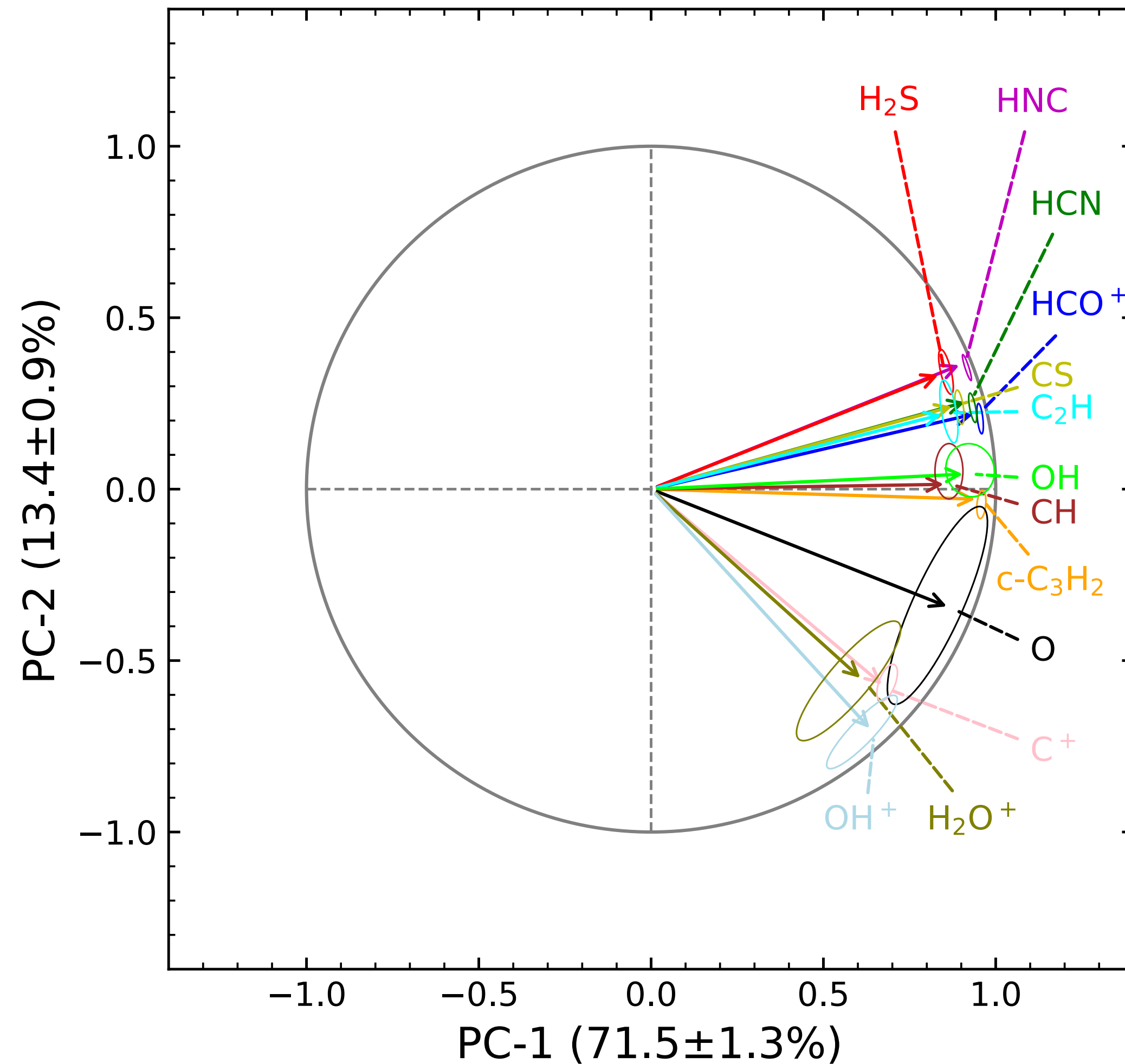
Correlations between species (hydrides and simple molecules)

20

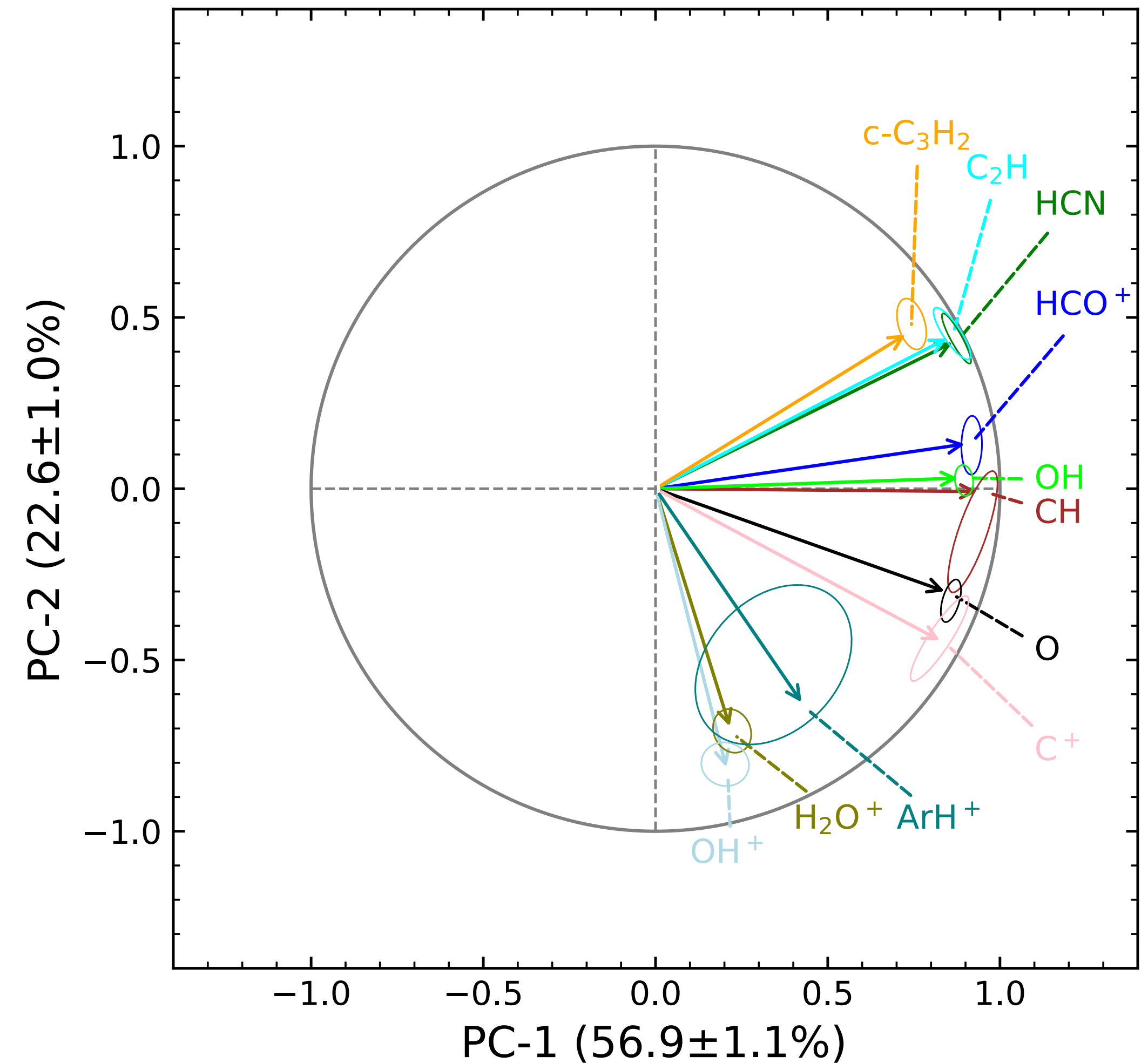
Similarity between two vectors of species
= the **cosine of the angle between the
vectors** ($\cos \theta = \mathbf{A} \cdot \mathbf{B} / \|\mathbf{A}\| \|\mathbf{B}\|$)

(HyGALII, Kim et al. 2023)

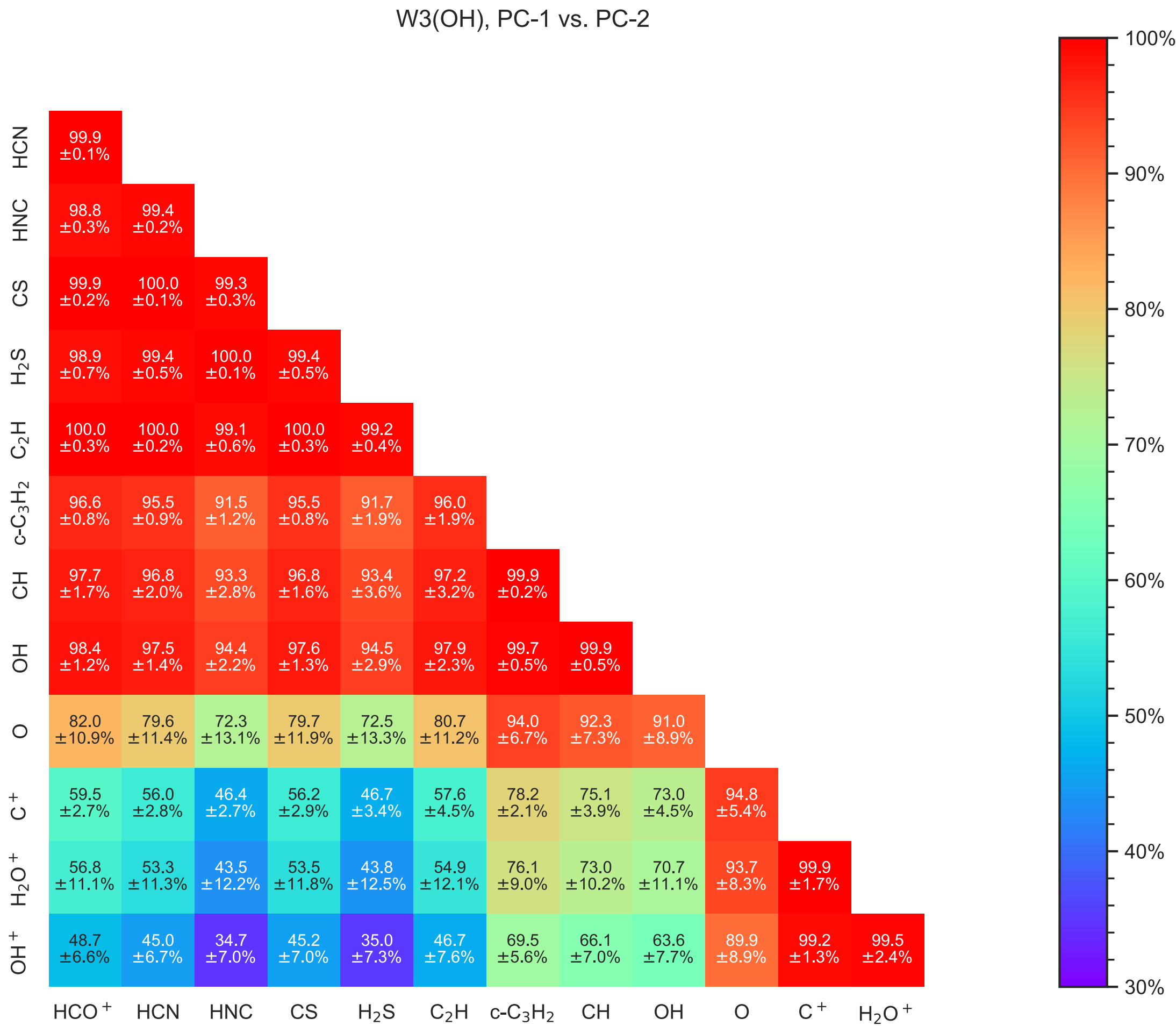
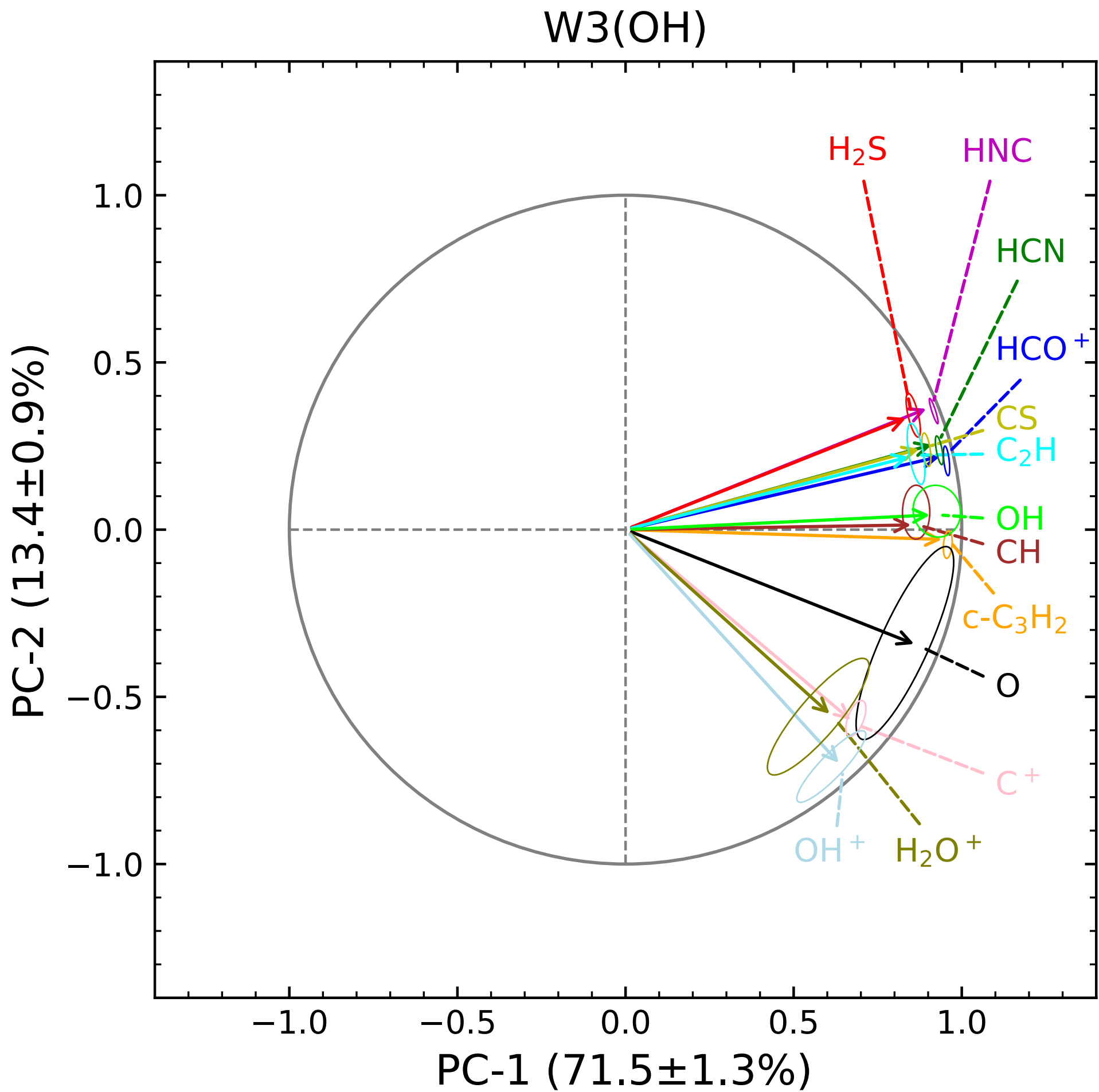
W3(OH)

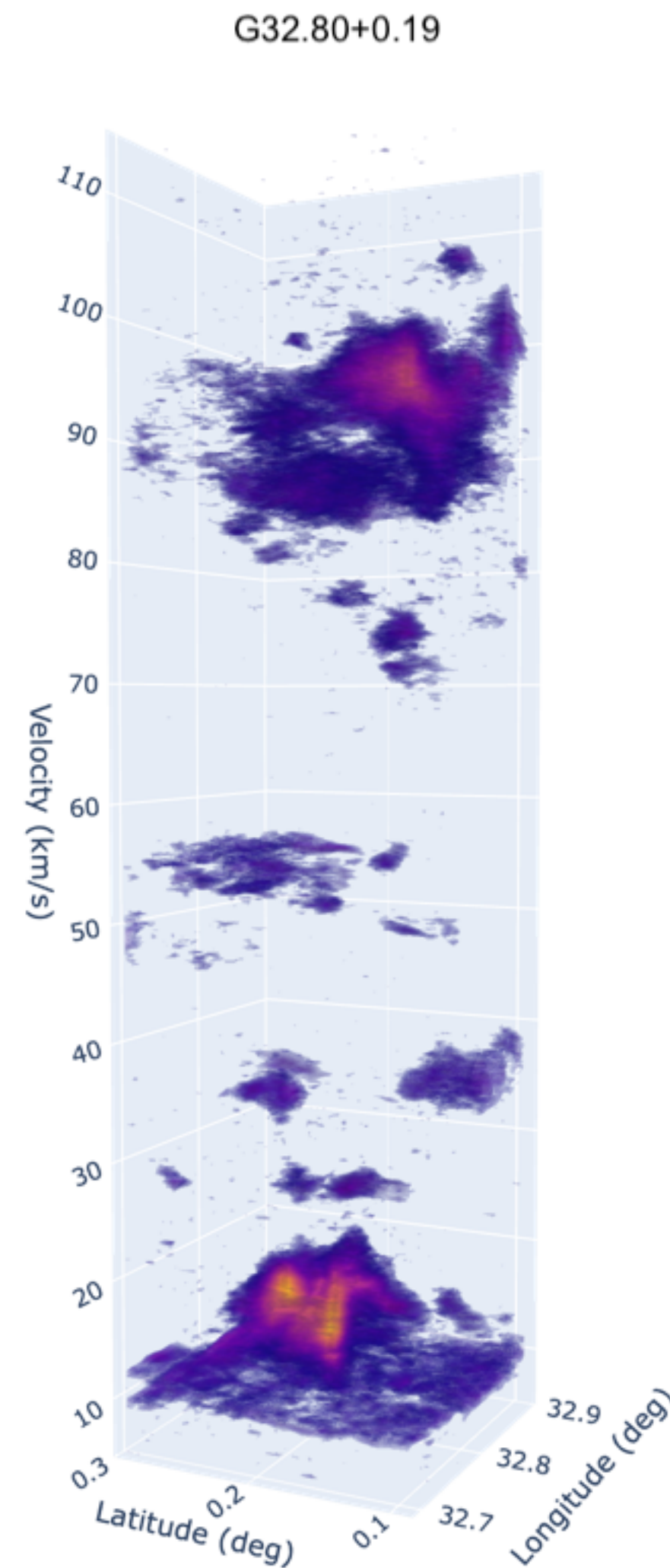


W3 IRS5



- 1. OH⁺, H₂O⁺ and ArH⁺, and C⁺ lie away from neutral molecular species HCN, HNC, CS, H₂S, C₂H, and c-C₃H₂, and HCO⁺.
- 2. The sulfur-bearing species, CS and H₂S, lie close to the neutral molecular species.
- 3. The vectors for CH and OH lie very close to each other.

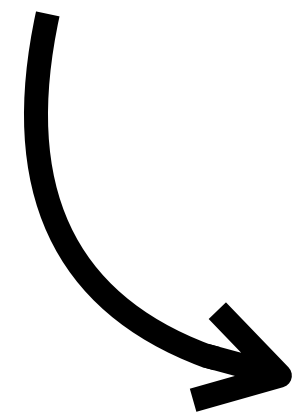




- The diffuse ISM is not homogenous - sub-structures exist within a cloud.
 - Such inhomogeneous structures make HCO⁺ and CCH less reliable tracers for H₂ gas!
- ➡ As we have seen, HCO⁺ does not correlate well with CH & OH for large velocity integrations toward Galactic diffuse and translucent clouds.
- Only relying on HCO⁺ and CCH might not give the full information of H₂.
- ➡ Thus, **CH & OH at 2 THz is still critical for diffuse ISM studies toward lines of sight in high visual extinctions**, as such Galactic lines of sight are important to understand the chemical and physical evolutions of galaxies.



- To investigate **how molecular clouds are formed** and **the chemical and physical processes** leading to the transitions from atomic to molecular gas by observing **hydrides, C⁺, and O**.



- Combining ancillary data acquired from ground-based telescopes with limited sightlines, we find different species have favor species groups — atomic or molecular dominant gas.
 - Group 1: HCO⁺, OH, and CH traces diffuse molecular gas.
 - Group 2: Ion-hydrides and C⁺ traces atomic gas.
 - Group 3: Atomic oxygen seems to be associated with the transition between atomic and molecular gas.

Analyzing the SOFIA data of the entire sample with the ancillary datasets will allow us to study the properties of the diffuse ISM and chemical/physical processes associated with the Milky Way structure.